NASA Contractor Report 181816

ICASE REPORT NO. 89-19

ICASE

THE INVISCID AXISYMMETRIC STABILITY OF THE SUPERSONIC FLOW ALONG A CIRCULAR CYLINDER

Peter W. Duck

Contract Nos. NAS1-18605, NAS1-18107
February 1989

INSTITUTE FOR COMPUTER APPLICATIONS IN SCIENCE AND ENGINEERING
NASA Langley Research Center, Hampton, Virginia 23665

Operated by the Universities Space Research Association

National Aeronautics and
Space Administration

Langley Research Center
Hampton, Virginia 23665

THE INVISCID AXISYMMETRIC STABILITY OF THE SUPERSONIC FLOW ALONG A CIRCULAR CYLINDER

Peter W. Duck[1]
Department of Mathematics,
University of Manchester.
Manchester, ENGLAND

Abstract

The supersonic flow past a thin straight circular cylinder is investigated. The associated boundary layer flow (i.e. the velocity and temperature field) is computed; the asymptotic, far downstream solution is obtained, and compared with the full numerical results.

The inviscid, linear, axisymmetric (temporal) stability of this boundary layer is also studied. A so called "doubly generalized" inflexion condition is derived, which is a condition for the existence of so called "subsonic" neutral modes. The eigenvalue problem (for the complex wavespeed) is computed for two freestream Mach numbers (2.8 and 3.8), and this reveals that curvature has a profound effect on the stability of the flow. The first unstable inviscid mode is seen to rapidly disappear as curvature is introduced, whilst the second (and generally the most important) mode suffers a substantially reduced amplification rate.

[1]This research was suppported by the National Aeronautics and Space Administration under NASA Contracts No. NAS1-18605 and NAS1-18107 while the author was in residence at the Institute for Computer Applications in Science and Engineering (ICASE), NASA Langley Research Center, Hampton, VA 23665

1. Introduction

The current and proposed development of high speed flight vehicles has rekindled the general research effort into supersonic and hypersonic flows. One of the key areas of aerodynamic study is that of boundary layer stability/transition to turbulence. In the case of compressible flow, Tollmien-Schlichting, Görtler and inviscid instabilities are all possible.

The problem of the stability of axisymmetric flows is of obvious relevance to flight vehicles, for example to the flow over fuselages and engine cowlings. In a recent paper Duck and Hall (1988a) used triple-deck theory to consider the linear (and weakly non-linear) viscous instability of an axisymmetric boundary layer in a supersonic flow to axisymmetric instabilities. It was found that viscous modes can exist in pairs (i.e. for a given body radius, there exist two neutral wavenumbers with two corresponding wavespeeds), and that at a given Mach number such modes occur only for a body radius less than a critical value (dependent on Mach number).

In a second paper, Duck and Hall (1988b) went on to consider non-axisymmetric disturbances. These were generally found to be more important than axisymmetric viscous modes (possessing generally larger growth rates and occuring at larger body radii), whilst again it was found that neutral modes existed in pairs at body radii less than some critical value (dependent on the Mach number and azimuthal wavenumber).

However it is generally found in the case of supersonic flows that inviscid disturbances are more important than viscous disturbances (this is in contrast to incompressible flows where viscous instabilities are generally dominant).

One of the earliest attempts to study inviscid compressible stability was made by Küchemann (1938); in this study, the temperature gradient

and the curvature of velocity profile (together with the effects of viscosity) were both neglected, assumptions which it turns out cannot be properly justified. The work that provided a key to understanding this type of instability was Lees and Lin (1946), in which a rational asymptotic approximation was developed, analogous to the incompressible work of Lin (1945). It was found that the quantity $\frac{\partial}{\partial y^*}\left[\rho^* \frac{\partial u^*}{\partial y^*}\right]$ (where u^* denotes the velocity tangential to the surface, y^* the coordinate normal to the surface, and ρ^* the fluid density) plays a key role, very similar to that of $\partial^2 u^*/\partial y^{*2}$ in incompressible theory, and as such may lead to a "generalised inflexion point" type of instability if this quantity is zero. It was shown that unlike incompressible Blasius type layers, the flat plate compressible boundary layer can be unstable to purely inviscid modes. This (two-dimensional) work on compressible boundary layer was then extended to three dimensions by Reshotko (1962).

However the major differences between incompressible and compressible theory were not fully uncovered until extensive numerical calculations were possible. The first of these, by Brown (1962), was followed by a series of computational studies by Mack (1963, 1964, 1965a,b, 1969, 1984, 1987). A further important difference with incompressible results was then revealed, namely that compressible theory predicts an infinite sequence of additional modes. These are referred to as higher modes, and are of great importance for boundary layers since it is the first of these (the so-called second mode) that is then most unstable according to inviscid theory.

In the light of this numerical work, the prediction of Lees (1947), that cooling the wall acts to stabilize the boundary layer, turns out to be a little misleading (cooling can actually destabilise the flow,

according to Mack 1969, 1984, 1987); in this case, although the "generalised inflexion point" of the profile may disappear with cooling, these additional modes persist.

In the light of this work on planar boundary layers, we now turn to consider the inviscid axisymmetric stability of the boundary layer on a straight circular cylinder, the generators of the cylinder lying parallel to the flow. In particular we wish to investigate the effect curvature plays on the stability of the flow, and so we postulate that (generally) the radius of the body is of the same order of thickness as the boundary layer. Consistent with this we choose to prescribe planar conditions at the "leading edge" of the cylinder, although the techniques to be described could be readily extended to other leading edge conditions (e.g. "rounded tips"). This approach may be fully justified if we restrict our attention to thin cylinders.

2. Equations of motion/state

We take the z^* axis to coincide with the axis of the cylinder, r^* the radial coordinate, and θ the azimuthal angle. a^* is the radius of the cylinder, which is taken to be independent of both z^* and θ. The velocity vector is taken to be $\underset{\sim}{v}^* = (v_1^*, v_2^*, v_3^*)$ in the (r^*, θ, z^*) directions respectively, and T^* to be the temperature of the fluid. Throughout we assume the flow to be completely independent of θ, and it is also assumed that the azimuthal velocity component $v_2^* = 0$. The (full) equations (in the cylindrical system) of continuity, momentum and energy, are, respectively (see Thompson 1972)

$$\frac{\partial \rho^*}{\partial t^*} + \frac{\partial}{\partial r^*}(\rho^* v_1^*) + \frac{\rho^* v_1^*}{r^*} + \frac{\partial}{\partial z^*}(\rho^* v_3^*) = 0, \tag{2.1}$$

$$\rho^* \frac{Dv_1^*}{Dt^*} = -\frac{\partial p^*}{\partial r^*} + \frac{\partial \Sigma_{r^* r^*}}{\partial r^*} + \frac{\partial \Sigma_{r^* z^*}}{\partial z^*} + \frac{1}{r}\Sigma_{r^* r^*}, \tag{2.2}$$

$$\rho^* \frac{Dv_3^*}{Dt^*} = -\frac{\partial p^*}{\partial z^*} + \frac{\partial \Sigma_{z^* r^*}}{\partial r^*} + \frac{\partial \Sigma_{z^* z^*}}{\partial z^*} + \frac{\Sigma_{z^* r^*}}{r^*}, \tag{2.3}$$

$$\rho^* \frac{D}{Dt^*}(c_p T^*) - \frac{Dp}{Dt^*} = \Gamma^* + \frac{1}{r^*}\frac{\partial}{\partial r^*}(K^* r^* \frac{\partial T^*}{\partial r^*}) + \frac{\partial}{\partial z^*}(K^* \frac{\partial T^*}{\partial z^*}). \tag{2.4}$$

Here ρ^* denotes the density of the fluid, p^* the pressure, c_p the specific heat at constant pressure, K^* the coefficient of heat conductivity. The Eulerian operator is defined as

$$\frac{D}{Dt^*} = \frac{\partial}{\partial t^*} + v_1^* \frac{\partial}{\partial r^*} + v_3^* \frac{\partial}{\partial z^*}, \tag{2.5}$$

and the viscous stress components (assuming Newtonian flow) are

$$\sum_{r^*r^*} = 2\mu^* \frac{\partial v_1^*}{\partial r^*} + \frac{2}{3}(\lambda^* - \mu^*)\,\nabla \cdot \underset{\sim}{v}^*, \tag{2.6}$$

$$\sum_{z^*z^*} = 2\mu^* \frac{\partial v_3^*}{\partial z^*} + \frac{2}{3}(\lambda^* - \mu^*)\,\nabla \cdot \underset{\sim}{v}^*, \tag{2.7}$$

$$\sum_{r^*z^*} = \sum_{z^*r^*} = \mu^* \left[\frac{\partial v_3^*}{\partial r^*} + \frac{\partial v_1^*}{\partial z^*}\right]. \tag{2.8}$$

The dispersion function Γ^* is defined to be

$$\Gamma^* = 2\mu^* \left[D^2_{r^*r^*} + D^2_{z^*z^*} + 2\,D^2_{z^*r^*}\right] + \frac{2}{3}(\lambda^* - \mu^*)\,(\nabla \cdot \underset{\sim}{v}^*), \tag{2.9}$$

where the rate-of-deformation tensors are

$$D_{r^*r^*} = \frac{\partial v_1^*}{\partial r^*}, \tag{2.10}$$

$$D_{z^*z^*} = \frac{\partial v_3^*}{\partial z^*}, \tag{2.11}$$

$$D_{r^*z^*} = \frac{1}{2}\left[\frac{\partial v_1^*}{\partial z^*} + \frac{\partial v_3^*}{\partial r^*}\right]. \tag{2.12}$$

μ^* denotes the first coefficient of viscosity, and λ^* the second coefficient of viscosity ($= 1.5 \times \mu^*$).

We now go on to assume a perfect gas equation of state, namely

$$p^* = \rho^* R^* T^*, \tag{2.13}$$

(where R^* is the gas constant). We also assume that μ^* is

solely a function of T^* (to be prescribed later).

The surface of the cylinder lies along $r^* = a^*$, $z^* > 0$, along which we assume $\underset{\sim}{v}^* = \underset{\sim}{0}$. We also assume the surface of the cylinder is insulated, and so

$$\left.\frac{\partial T^*}{\partial r^*}\right|_{r^*=a^*} = 0. \tag{2.14}$$

Conditions at $z = 0$ must be specified. For the purposes of this paper, we assume that the boundary layer at $z = 0$ has zero thickness (implying planar conditions prevail); a similar assumption was made by Seban and Bond (1951) and their comments regarding this assumption are valid here. Further, since the cylinder is taken to be straight and thin, to leading order the far field is taken to be uniform, with velocity vector $(0, 0, U_\infty^*)$. The problem is now finally closed, and in the following section we go on to consider the basic boundary layer flow on the surface of the cylinder, obtained by an approximation of the governing equations detailed above.

3. The basic flow.

3.1 The boundary layer approximation

Here we consider the steady boundary layer approximation for the basic flow, derived from equations (1.1) - (1.4). A fundamental (and important) component of this paper is the inclusion of curvature terms in the governing equations; we achieve this by generally taking the body radius to be of the same order as the boundary layer thickness (a similar approach was adopted by, for example, Seban and Bond 1951, Glauert and Lighthill 1955, Stewartson 1955, Bush 1976 and Duck and Bodonyi 1986).

With the formation of a thin boundary layer, (comparable in thickness to the body radius) we expect the following classical assumptions to hold

$$\frac{\partial}{\partial r^*} >> \frac{\partial}{\partial z^*} , \tag{3.1}$$

and

$$v_3^* >> v_1^*, \tag{3.2}$$

(these orders will be made more precise shortly). Equations (1.1)-(1.4) then reduce to

$$\frac{\partial}{\partial r^*}(\rho^* v_1^*) + \frac{\rho^* v_1^*}{r^*} + \frac{\partial}{\partial z^*}(\rho^* v_3^*) = 0, \tag{3.3}$$

$$\frac{\partial p^*}{\partial r^*} = 0, \tag{3.4}$$

$$\rho^*\left[v_1^* \frac{\partial v_3^*}{\partial r^*} + v_3^* \frac{\partial v_3^*}{\partial z^*}\right] = \frac{1}{r^*}\frac{\partial}{\partial r^*}\left[r^*\mu^* \frac{\partial v_3^*}{\partial r^*}\right], \tag{3.5}$$

$$c_p\rho^*\left[v_1^* \frac{\partial T^*}{\partial r^*} + v_3^* \frac{\partial T^*}{\partial z^*}\right] = \mu^*\left[\frac{\partial v_3^*}{\partial r^*}\right]^2 + \frac{1}{r^*}\frac{\partial}{\partial r^*}\left[K^* r^* \frac{\partial T^*}{\partial r^*}\right]. \tag{3.6}$$

The last of these equations assumes c_p to be a constant. Notice that the pressure is everywhere uniform on account of (3.4), together with our inherent assumption that the body radius is of the same order as the boundary layer thickness, i.e. very thin.

One important consequence of (3.4) is that the equation of state may be written in the following form

$$\rho^* T^* = \rho_\infty^* T_\infty^*, \tag{3.7}$$

where subscript ∞ denotes freestream conditions.

It is now convenient to introduce non-dimensional quantities $(v_1, v_3, r, z, T, \rho, \mu)$

$$= (\mathrm{Re}\ v_1^*/U_\infty^*, v_3^*/U_\infty^*, r^*/a,\ \mathrm{Re}^{-1} z^*/a,\ T^*/T_\infty^*,\ \rho^*/\rho_\infty^*\ \mu^*/\mu_\infty^*), \tag{3.8}$$

where Re is the Reynolds number, based on body radius a^*, namely

$$\mathrm{Re} = \frac{U_\infty^*\ a^* \rho_\infty^*}{\mu_\infty^*}, \tag{3.9}$$

which must be assumed large if the assumptions (3.1) and (3.2) are to be valid.

Equations (3.3) - (3.6) may then be written in the following non-dimensional form

$$\frac{\partial}{\partial r}\left[\frac{v_1}{T}\right] + \frac{v_1}{rT} + \frac{\partial}{\partial z}\left[\frac{v_3}{T}\right] = 0, \tag{3.10}$$

$$\frac{\partial p}{\partial r} = 0, \tag{3.11}$$

$$v_1 \frac{\partial v_3}{\partial r} + v_3 \frac{\partial v_3}{\partial z} = \frac{T}{r} \frac{\partial}{\partial r}\left[r\ \mu \frac{\partial v_3}{\partial r}\right], \tag{3.12}$$

$$v_1 \frac{\partial T}{\partial r} + v_3 \frac{\partial T}{\partial z} = \mu T(\gamma-1) M_\infty^2 \left[\frac{\partial v_3}{\partial r}\right]^2 + \frac{T}{r} \frac{\partial}{\partial r}\left[\frac{r\mu}{\sigma} \frac{\partial T}{\partial r}\right]. \tag{3.13}$$

Here σ is the Prandtl number, namely

$$\sigma = \frac{\mu^* c_p}{k^*}, \tag{3.14}$$

which in this paper we shall assume to be a constant; γ is the ratio of specific heats, and M_∞ the Mach number, namely

$$M_\infty = U_\infty^* / (\gamma R^* T_\infty^*)^{\frac{1}{2}}. \tag{3.15}$$

The boundary conditions are

$$\left.\frac{\partial T}{\partial r}\right|_{r=1} = 0,$$

$$v_1 = v_3 = 0 \quad \text{on} \quad r = 1,$$

$$\left.\begin{aligned} v_3 &\to 1 \\ T &\to 1 \end{aligned}\right\} \quad \text{as} \quad r \to \infty. \tag{3.16}$$

To close the problem formally, we require a relationship linking μ to T. Here we take the simplest form, namely the linear Chapman law (Stewartson 1964),

$$\mu = T, \tag{3.17}$$

although, here, conceptually, there would be no difficulty incorporating a more complex viscosity/temperature law.

3.2 Numerical solution

As $z \to 0$ we specify (i) the solution approaches planar conditions (Stewartson 1964) and so we expect the solution to become singular. This latter condition renders the problem in its present form inappropriate for numerical treatment. Instead we write

$$v_1 = \zeta^{-1}\,\hat{v}_1\,(\eta,\zeta),$$

$$v_3 = \hat{v}_3\,(\eta,\zeta),$$

$$T = \hat{T}\,(\eta,\zeta), \tag{3.18}$$

with $\zeta = z^{\frac{1}{2}}$, (3.19a)

$$\eta = (r-1)/\zeta. \tag{3.19b}$$

The "hatted" functions are now expected to be completely regular as $\zeta \to 0$, approaching their planar counterparts. Equations (3.10), (3.12), (3.13) then become, respectively

$$\hat{T}\,\hat{v}_{1\eta} - \hat{v}_1\,\hat{T}_\eta - \tfrac{1}{2}\,\eta\hat{T}\,\hat{v}_{3\eta} + \tfrac{1}{2}\,\hat{\zeta}\hat{T}v_{3\zeta}$$

$$+ \tfrac{1}{2}\,\eta\hat{T}_\eta\,\hat{v}_3 - \tfrac{1}{2}\hat{\zeta}v_3\,\hat{T}_\zeta + \frac{\hat{\zeta}\hat{T}\hat{v}_1}{1+\eta\zeta} = 0, \tag{3.20}$$

$$\hat{v}_1\hat{v}_{3\eta} - \tfrac{1}{2}\,\eta\,\hat{v}_3\,\hat{v}_{3\eta} + \tfrac{1}{2}\,\hat{\zeta}\hat{v}_3\hat{v}_{3\zeta}$$

$$- \hat{T}^2\left[v_{3\eta\eta} + \frac{\zeta\hat{v}_{3\eta}}{1+\zeta\eta}\right] + \hat{T}\,\frac{\partial\hat{T}}{\partial\eta}\,\hat{v}_{3\eta}, \tag{3.21}$$

$$\hat{v}_1\,\hat{T}_\eta - \frac{1}{2}\,\eta\,\hat{v}_3\,\hat{T}_\eta + \frac{1}{2}\,\zeta\,\hat{T}_\zeta\,\hat{v}_3 = \hat{T}^2(\gamma-1)M_\infty^2(\hat{v}_{3\eta})^2$$

$$+ \frac{\hat{T}}{\sigma}\,(\hat{T}_\eta)^2 + \frac{\hat{T}^2}{\sigma}\,\hat{T}_{\eta\eta} + \frac{\hat{T}^2\zeta}{\sigma(1+\zeta\eta)}\,\hat{T}_\eta, \tag{3.22}$$

subject to

$$\hat{T}_\eta = 0 \quad \text{on} \quad \eta = 0,$$

$$\hat{v}_1 = \hat{v}_3 = 0 \quad \text{on} \quad \eta = 0,$$

$$\hat{T} \to 1 \quad \text{as} \quad \eta \to \infty,$$

$$\hat{v}_3 \to 1 \quad \text{as} \quad \eta \to \infty. \tag{3.23}$$

It is possible to define a streamfunction which would ensure the continuity equation (3.20) is always satisfied; however in this case, in addition to the order of the momentum equation being increased, the coefficients of the equations become considerably more complicated. Further, it does not appear possible to introduce a Howarth-Dorodnitsyn (Stewartson 1951, Moore 1951) like transformation which in the planar case considerably simplifies the governing equations. For this reason it was decided to seek a numerical solution to $\hat{v}_1$, $\hat{v}_3$ and $\hat{T}$ directly. Notice setting $f = 0$ reduces the system (3.20) - (3.23) to the planar problem, namely the ordinary-differential system

$$\hat{T}\,\hat{v}_{1\eta} - \hat{v}_1\,\hat{T}_\eta - \tfrac{1}{2}\eta\,\hat{T}\,\hat{v}_{3\eta} + \tfrac{1}{2}\,\eta\hat{T}_\eta\hat{v}_3 = 0, \tag{3.24}$$

$$\hat{v}_1\,\hat{v}_{3\eta} - \frac{1}{2}\,\eta\hat{v}_3\,\hat{v}_{3\eta} = \hat{T}^2\,\hat{v}_{3\eta\eta} + \hat{T}\,\hat{T}_\eta\hat{v}_{3\eta}, \tag{3.25}$$

$$\hat{v}_1\,\hat{T}_\eta - \frac{1}{2}\,\eta\hat{v}_3\,\hat{T}_\eta = \hat{T}^2\,(\gamma-1)M_\infty^2\,(\hat{v}_{3\eta})^2 + \frac{\hat{T}^2}{\sigma}\,\hat{T}_{\eta\eta} + \frac{\hat{T}}{\sigma}\,(\hat{T}_\eta)^2, \tag{3.26}$$

(again subject to (3.23)).

The variables

$$\hat{v}_3^1 = \hat{v}_{3\eta},$$

$$\hat{T}^1 = \hat{T}_\eta, \tag{3.27}$$

were introduced, and the system (3.24) - (3.26) together with (3.27) were written as a system of first order ordinary differential equations, which were then approximated by second-order finite differences. The truncated system was then solved by means of Newton iteration. At each iteration level, the algebraic system was of block-diagonal form, with each block comprising 10x5 elements.

Once the above solution was obtained, the system (3.20) - (3.23) was treated in much the same way, with a Crank-Nicolson approximation being used to approximate ξ derivatives (again the problem was treated as a system of first order equations in η). In this way, the solution was extended forwards in ξ.

Fig. 1a shows the distribution of $\xi^{-1}\,\hat{v}_{3\eta}\,(\eta{=}0)$ with ξ, and Fig. 1b the corresponding distribution of $\hat{T}(\eta{=}0)$. These results are for $M_\infty = 2.8$, with fluid constants $\sigma = 0.72$, $\gamma = 1.4$. The $\xi^{-1}\hat{v}_{3\eta}\,(\eta{=}0)$ distribution is singular in the planar limit as $\xi \to 0$, and then appears to (slowly) fall continuously as ξ increases. The $\hat{T}(\eta{=}0)$ distribution declines slightly from its planar value at $\xi{=}0$.

Results for $M_\infty = 3.8$ (same fluid constants as above) are shown in Fig. 2a ($\xi^{-1}\hat{v}_3(\eta{=}0)$ distribution) and Fig. 2b ($\hat{T}(\eta{=}0)$ distribution); these suggest the same basic characteristics as the lower Mach number results.

The limit as $\xi \to \infty$ is of some interest. Although, as indicated earlier, the incompressible case in this limit is well documented, the particular details for the compressible case do not appear to have been described, although Stewartson (1964) speculates that a similar approach to the incompressible case is necessary. In the following sub-section we show this is indeed the case.

3.3 The far downstream flow

We find it convenient to reconsider the system (3.10) - (3.13) (together with (3.17)) when studying the limit of $z \to \infty$. The incompressible work of Glauert and Lighthill (1955), Stewartson (1955) and Bush (1976) suggests that two radial lengthscales are important in this limit, namely $r = O(1)$ and $r = O(z^{\frac{1}{2}})$. Following these earlier works, we find it convenient to define the parameter

$$\epsilon = (\tfrac{1}{2} \log z)^{-1}, \qquad (3.28)$$

$$= (\log \zeta)^{-1}$$

which is necessarily small as $z \to \infty$.

Guided partly by the incompressible case, we expect the solution for $r = O(1)$ to take the following form

$$v_1 = O(1/\zeta), \qquad (3.29a)$$

$$v_3 = \bar{v}_3(r,\zeta) + O(1/\zeta), \qquad (3.29b)$$

$$T = \bar{T}_0(r,\zeta) + O(1/\zeta), \qquad (3.29c)$$

where "barred" quantities are expected to be generally order one. Subsitution of (3.29) into (3.10) - (3.13) immediately reveals the result (neglecting $O(1/\zeta)$ terms)

$$\frac{\partial}{\partial r}\left[r\bar{T}_0 \frac{\partial \bar{v}_3}{\partial r}\right] = 0, \qquad (3.30)$$

and

$$\bar{T}_0(\gamma-1)M_\infty^2\epsilon^2\left[\frac{\partial \bar{v}_3}{\partial r}\right]^2 + \frac{1}{r}\frac{\partial}{\partial r}\left[r\,\frac{\bar{T}_0}{\sigma}\frac{\partial \bar{T}_0}{\partial r}\right] = 0. \qquad (3.31)$$

Integrating (3.30) yields

$$\bar{T}_0 \frac{\partial \bar{v}_3}{\partial r} = \frac{\bar{K}}{r}, \tag{3.32}$$

where $\bar{K}$ is independent of r. Substitution of (3.32) into (3.31) yields

$$\bar{T}_0 \frac{\partial}{\partial r}\left[r\bar{T}_0 \frac{\partial T_0}{\partial r}\right] + \frac{(\gamma-1)\bar{K}^2 M_\infty{}^2 \epsilon^2 \sigma}{r} = 0. \tag{3.33}$$

To facilitate the solution to (3.33) we write

$$\bar{r} = \ln r, \tag{3.34}$$

and so

$$\bar{T}_0 \frac{\partial}{\partial \bar{r}}\left[\bar{T}_0 \frac{\partial \bar{T}_0}{\partial \bar{r}}\right] + \bar{K}^2 \sigma M_\infty{}^2 (\gamma-1)\epsilon^2 = 0. \tag{3.35}$$

This equation is further simplified by the use of a second transformation

$$\bar{R} = \int \frac{d\bar{r}}{\bar{T}_0}, \tag{3.36}$$

giving

$$\frac{\partial^2 \bar{T}_0}{\partial \bar{R}^2} + \bar{K}^2 M_\infty{}^2 \sigma(\gamma-1)\epsilon^2 = 0. \tag{3.37}$$

Consequently

$$\bar{T}_0 = -\frac{\bar{K}^2}{2} M_\infty{}^2 \sigma(\gamma-1)\epsilon^2 \bar{R}^2 + \epsilon A_0 \bar{R} + B_0, \tag{3.38}$$

where A_0 and B_0 are independent of $\bar{R}$.

Before proceding further with this solution, we consider next the outer solution where $\eta = 0(1)$. Guided by the above, and also again the corresponding incompressible results, we expect the solution to develop as

$$v_3 = 1 + \epsilon\tilde{v}_3(\bar{\eta}) + O(\epsilon^2),$$

$$T = 1 + \epsilon\tilde{T}_3(\bar{\eta}) + O(\epsilon^2),$$

$$v_1 = \epsilon\tilde{v}_1(\bar{\eta}) + O(\epsilon^2), \tag{3.39}$$

where we have written,

$$\bar{\eta} = \int_0^{\eta} \frac{d\eta}{\bar{T}}, \tag{3.40}$$

and also we have implemented freestream conditions on v_3 and T.

If $\bar{T}_0(r,\bar{s})$ is to match correctly to (3.39), we must have (to leading order)

$$A_0 + B_0 - \tfrac{1}{2}\bar{K}^2 M_\infty^2(\gamma-1)\sigma = 1, \tag{3.41}$$

(it is now clear that although the first term on the right-hand-side of (3.38) is notionally $O(\epsilon^2)$, its inclusion is essential for a correct matching process, as is the second term). Note that we have used the result

$$\bar{R} \sim \bar{r} - \ln r \quad \text{as} \quad r \to \infty. \tag{3.42}$$

The matching of $\tilde{v}_3(r,\bar{s})$ with the outer solution is achieved by setting $\bar{K} = 1$.

The $O(\epsilon)$ corrections to (3.39) are then given by

$$\tilde{v}_3(\bar{\eta}) = \int_{\infty}^{\bar{\eta}} e^{-\frac{1}{2}\int\frac{\eta}{\bar{T}}d\bar{\eta}}\, d\bar{\eta}, \tag{3.43}$$

and

$$\tilde{T}_1(\bar{\eta}) = [A_0 - \sigma(\gamma-1)M_\infty^2]\int_{\infty}^{\bar{\eta}} e^{-\frac{\sigma}{2}\int\frac{\eta}{\bar{T}}d\bar{\eta}}\, d\bar{\eta}. \tag{3.44}$$

Both $\bar{\eta}$ and $\bar{R}$ may be regarded as forms of "optimal coordinates", as their use is essential for the correct matching of solutions.

To complete the problem, we now require to specify conditions on $r = 1$. In the insulated wall case, to which the bulk of this paper is devoted, we require

$$\left.\frac{\partial T}{\partial r}\right|_{r=1} = 0, \tag{3.45}$$

and so $A_0 = 0$, (3.46)

and this implies that

$$T_0\big|_{r=1} = 1 + \frac{\sigma}{2}(\gamma-1)M_\infty{}^2 + O(\epsilon), \tag{3.47}$$

which implies

$$\left.\frac{\partial \bar{v}_3}{\partial r}\right|_{r=1} = -\frac{1}{1 + \frac{\sigma}{2}(\gamma-1)M_\infty{}^2} + O(\epsilon), \tag{3.48}$$

(on account of (3.32)).

These asymptotic results are indicated as broken lines on Figs. 1 and 2 for comparison with the full numerical results; the agreement is satisfactorily given the relative "largeness" of the small parameter ϵ.

If on the other hand the surface of the cylinder is heated or cooled, i.e. $T\big|_{r=1}$ is specified (to be T_w say), then we must have

$$B_0 = T_w, \tag{3.49}$$

and so to leading order

$$A_0 = 1 + \frac{1}{2}\sigma(\gamma-1)M_\infty{}^2 - T_w, \tag{3.50}$$

giving

$$\left.\frac{\partial \bar{T}_0}{\partial r}\right|_{r=1} = \frac{\epsilon}{\bar{T}_w}\left[1 + \frac{1}{2}\sigma(\gamma-1)M_\infty{}^2 - T_w\right] + O(\epsilon^2), \tag{3.51}$$

together with,

$$\left.\frac{\partial \bar{v}_3}{\partial r}\right|_{r=1} = \frac{1}{\bar{T}_w} + O(\epsilon). \tag{3.52}$$

In the following section we turn our attention to the inviscid instability of flows corresponding to the insulated wall class.

4. Inviscid disturbances

4.1 Disturbance equations

We now seek to determine the effect of a small amplitude disturbance on the basic flow described in the previous section, to determine whether growth/instability can occur. We impose a disturbance whose wavelength is generally comparable to that of the boundary layer thickness and therefore also of the body radius $(O(a^*))$, in which case the parallel flow approximation can be fully justified; this implies the disturbance equations are all inviscid.

Specifically, at a fixed z station, we write

$$v_1^* = \delta\bar{\alpha}U_\infty^* \; \bar{v}(r) \; e^{i\bar{\alpha}(Z-ct)} \tag{4.1}$$

$$v_3^* = U_\infty^* \left[w_0(r) + \delta\tilde{w}(r)e^{i\bar{\alpha}(Z-ct)}\right], \tag{4.2}$$

$$T^* = T_\infty^*\left[T_0(r) + \delta\tilde{T}(r) \; e^{i\bar{\alpha}(Z-ct)}\right], \tag{4.3}$$

$$\rho^* = \rho_\infty^* \left[\frac{1}{T_0(r)} + \delta\tilde{\rho}(r) \; e^{i\bar{\alpha}(Z-ct)}\right], \tag{4.4}$$

$$p^* = \rho_\infty^* R^* T_\infty^* \left[1 + \delta\tilde{p}(r)e^{i\bar{\alpha}(Z-ct)}\right], \tag{4.5}$$

where δ is some small (disturbance amplitude) parameter,

$$t = (U_\infty^*/a^*)t^*,$$

$$Z = z^*/a^*,$$

and so the $Z = O(1)$ scale is very much shorter than the $z = O(1)$

scale, $\bar{\alpha}$ is the non-dimensional spatial wavenumber, and c the the non-dimensional wavespeed, and

$$w_0(r) = \hat{v}_3(r,z),$$

$$T_0(r) = \hat{T}(r,z), \tag{4.6}$$

where $\hat{v}_3$ and $\hat{T}$ are as defined in Section 3.

Substituting (4.1) - (4.4) into (1.1) - (1.4), (1.13), taking the $O(\delta)$ terms with the highest order in R yields the following disturbance equations

$$-i\,c\tilde{\rho} + \frac{i\tilde{w}}{T_0} + \frac{1}{T_0 r}\,\tilde{v} + \frac{1}{T_0}\,\tilde{v}_r + iw_0\tilde{\rho} + \tilde{v}\,\frac{d}{dr}\left(\frac{1}{T_0}\right) = 0, \tag{4.7}$$

$$-\frac{ic}{T_0}\,\tilde{w} + \frac{iw_0\tilde{w}}{T_0} + \frac{\tilde{v}w_{0r}}{T_0} = -\frac{i\tilde{p}}{\gamma M_\infty^2}, \tag{4.8}$$

$$-\frac{i\tilde{\alpha}^2 c}{T_0}\,\tilde{v} + i\,\frac{\alpha^2 w_0\tilde{v}}{T_0} = \frac{-1}{\gamma M_\infty}\,2\tilde{p}_r, \tag{4.9}$$

$$\frac{1}{T_0}\left[-ic\tilde{T} + iw_0\,\tilde{T} + \tilde{v}T_{0r}\right] + \left[\frac{\gamma-1}{\gamma}\right]\left[ic\tilde{p} - iw_0\tilde{p}\right] = 0, \tag{4.10}$$

together with the disturbance equation of state

$$\tilde{p} = T_0\,\tilde{\rho} + \frac{\tilde{T}}{T_0}. \tag{4.11}$$

After some algebra the system reduces to the following two equations

$$\tilde{v}_r + \frac{\tilde{v}}{r} - \frac{w_{0r}\tilde{v}}{w_0-c} = \frac{i\bar{\alpha}\tilde{p}}{\gamma M_\infty^2}\left[\frac{T_0-M_\infty^2(w_0-c)^2}{w_0-c}\right], \tag{4.12}$$

$$\frac{i\bar{\alpha}^2(w_0-c)}{T_0}\,\tilde{v} = -\frac{\tilde{p}_r}{\gamma M_\infty^2}. \tag{4.13}$$

It was shown in the previous section that the appropriate scale as $z \to 0$ is η (see (3.19b)) rather than r. Consequently we find it convenient to use η however, rather than r, and also to introduce a scaled radial velocity component φ, and wavenumber α by

$$\tilde{v} = \zeta\varphi, \quad \bar{\alpha} = \alpha/\zeta$$

and so

$$\varphi_\eta + \frac{\zeta}{1+\zeta\eta}\,\varphi - \frac{w_{0\eta}\varphi}{w_0-c} = \frac{i\bar{\alpha}\tilde{p}}{\gamma M_\infty^2}\left[\frac{T_0-M_\infty^2(w_0-c)^2}{w_0-c}\right], \tag{4.14}$$

$$\frac{i\alpha^2(w_0-c)}{T_0}\,\varphi = \frac{-\tilde{p}_\eta}{\gamma M_\infty^2}. \tag{4.15}$$

Equations (4.14) and (4.15) may be combined to give

$$\frac{d}{d\eta}\left[\frac{(w_0-c)(\varphi_\eta + \frac{\zeta}{1+\zeta\eta}\,\varphi) - w_{0\eta}\,\varphi}{T_0 - M_\infty^2\,[w_0-c]^2}\right] = \frac{\alpha^2}{\bar{T}_0}\,(w_0-c)\varphi. \tag{4.16}$$

This equation is very similar to the well-known planar inviscid equation (Lees and Lin 1946, Reshotko 1962, Mack 1984, for example), except for the inclusion of the single curvature term, on the left-hand-side of the equation; notice that allowing $\zeta \to 0$ retrieves

the planar result.

On $\eta = 0$, we require

$$\varphi(\eta=0) = 0 \tag{4.17}$$

(the impermeability condition). The second condition is that φ is bounded as $\eta \to \infty$. This is achieved by taking the $\eta \to \infty$ limit of (4.16), i.e.

$$\varphi_{\eta\eta} + \frac{\zeta\varphi_\eta}{1+\zeta\eta} - \frac{\zeta^2\varphi}{(1+\zeta\eta)^2} = \alpha^2[1-M_\infty{}^2(1-c)^2]\varphi, \tag{4.18}$$

giving

$$\varphi \sim \varphi_\infty K_1\{\pm\alpha[1-M_\infty{}^2(1-c)^2]^{\frac{1}{2}}(\tfrac{1}{\zeta} + \eta)\}, \tag{4.19}$$

where $K_n(z)$ denotes the modified Bessel function of order n, argument z, and the sign is chosen such that the real part of the argument is positive to ensure boundedness as $\eta \to \infty$; φ_∞ is a constant. Equation (4.19) also leads to

$$p \sim \mp \frac{\varphi_\infty M_\infty{}^2 \; i\alpha \; (1-c) K_0\{\pm\alpha[1-M_\infty{}^2(1-c)^2]^{\frac{1}{2}}(\frac{1}{\zeta} + \eta)\}}{[1-M_\infty{}^2(1-c)^2]^{\frac{1}{2}}}. \tag{4.20}$$

The eigenvalue problem (for the temporal case as considered here)

is then, for a given α, to find c subject to boundedness as $\eta \to \infty$, and such that the impermeability condition (4.17) is satisfied.

Before carrying out a detailed numerical study of this above eigenvalue problem, we turn to study an important sufficiency condition relating to the existence of certain unstable eigensolutions.

5. The doubly generalised inflexion condition

In the case of compressible planar flows, the existence of the so called generalised inflexion point, where (in our notation)

$$\frac{d}{d\eta}\left[\frac{w_0\eta}{T_0}\right] = 0, \tag{5.1}$$

is of great importance, as shown originally by Lees and Lin (1946) and confirmed by Reshotko (1962), Mack (1984, 1987) for example.

If condition (5.1) is satsified at some point η_i, then there exists a neutral solution, with wavespeed c, such that

$$c = w_0(\eta_i), \tag{5.2}$$

provided $T_0 - M_\infty^2 (w_0-c)^2 > 0,$ (5.3)

for all η.

This is a sufficient condition for the existence of a so called neutral subsonic disturbance, i.e. for which

$$1 - {}^1/_{M_\infty} < c < 1 + {}^1/_{M_\infty}, \tag{5.4}$$

using the terminology described by Mack (1984), where sonic disturbances have

$$c = 1 \pm {}^1/_{M_\infty}, \tag{5.5}$$

and supersonic disturbances have

$$c < 1 - {}^1/_{M_\infty}. \tag{5.6}$$

The condition (5.1) has a further important repurcussion, namely that a sufficient condition for the existence of an amplified disturbance is that

$$\frac{d}{d\eta}\left[\frac{w_0\eta}{T_0}\right] = 0 \tag{5.7}$$

at some $\eta > \eta_1$, where η_1 is the point at which

$$w_0(\eta) = 1 - {}^1/_{M_\infty}. \tag{5.8}$$

The question then arises, what is the effect of curvature on these important conditions? We address this question next. We take equation (4.16) as our starting point, and follow the general approach adopted in the past to tackle inflexional instabilities arising in planar compressible flows (eg. Mack 1984), although here the situation is more complicated because of the inclusion of curvature terms.

Taking equation (4.16), dividing through by w_0-c, and multiplying by φ^* (where an asterisk denotes a complex conjugate) we obtain

$$\frac{\varphi^*}{w_0-c}\frac{d}{dr}\left[\frac{(w_0-c)\ (\varphi_r + \frac{1}{r}\varphi_r) - w_{0_r}\varphi}{\chi}\right] = \frac{\bar{\alpha}^2}{T_0}\varphi\varphi^* \tag{5.9}$$

where $r = 1 + \zeta\eta$, (5.10)

and $$\chi = T_0 - M_\infty^2(w_0-c)^2. \tag{5.11}$$

If we now subtract the complex conjugate of (5.9) from (5.9) we obtain

$$\frac{\varphi^*}{w_0-c}\ \frac{d}{dr}\left[\frac{(w_0-c)(\varphi_r + \frac{1}{r}\ \varphi) - w_{0r}\varphi}{\chi}\right] - \frac{\varphi}{w_0-c^*}\frac{d}{dr}\left[\frac{(w_0-c^*)\ (\varphi_r^* + \frac{1}{r}\varphi^*) - w_{0r}\varphi^*}{\chi^*}\right]. \tag{5.12}$$

After some algebra, this may be written as follows

$$\varphi^*\frac{d}{dr}\left[\frac{\varphi_r + \frac{1}{r}\varphi}{\chi}\right] - \varphi\frac{d}{dr}\left[\frac{\varphi_r^* + \frac{1}{r}\varphi^*}{\chi^*}\right] = r\varphi\varphi^*\left\{\frac{1}{w_0-c}\frac{d}{dr}\left[\frac{w_{0r}}{\chi r}\right] - \frac{1}{w_0-c^*}\frac{d}{dr}\left[\frac{w_{0r}}{\chi^* r}\right]\right\} \tag{5.13}$$

We now focus attention on the limit of the neutral state, i.e. if

$$c = c_r + ic_i$$

then $c_i \to 0$. (5.14)

We may write $\chi^* = \chi$ in this limit without any difficulty (assuming the wave is not given by either of (5.5), which we shall see is outside of the scope of the following, anyway). However we exert some care in the treatment of the right hand-side of equation (5.13), which we now write as

$$\frac{1}{r}\frac{d}{dr}\left[\frac{r\varphi^*(\varphi_r + \frac{1}{r}\varphi) - r\varphi(\varphi_r^* + \frac{1}{r}\varphi^*)}{\chi}\right] = \frac{2ir|\varphi|^2 ic_i}{|w_0-c|^2}\frac{d}{dr}\left[\frac{w_{0r}}{\chi r}\right]. \quad (5.15)$$

We now use the following arguments: (i) as $c_i \to 0$, the derivative of the term in parentheses on the left-hand-side of (5.15) is always zero, except possibly at the point, r_i, where $w_0 = c$; (ii) the term inside the parentheses must be zero at the wall $(r = 1)$, and asymptote to zero at infinity <u>if the wave is subsonic</u>; (iii) the right-hand-side acts as a delta function at r_i as $c_i \to 0$, unless

$$\frac{d}{dr}\left[\frac{w_{0r}}{T_0 r}\right]_{r=r_i} = 0, \quad (5.16)$$

or equivalently

$$\frac{d}{d\eta}\left[\frac{w_{0\eta}}{T_0(1+\delta\eta)}\right]_{\eta=\eta_i} = 0, \quad (5.17)$$

where $\eta_i = (r_i-1)/\delta$. (5.18)

(note $\chi(r = r_i) = T_0$). This condition is clearly required in order to avoid a finite jump in the term in parentheses on the left-hand-side of (5.15), and the subsequent contradiction. Equation (5.16) is a

"doubly generalised inflexion condition", and includes a curvature term, not present in planar studies.

We thus see that (5.16) is a necessary and sufficient condition for the existence of so-called subsonic modes. In the following section we carry out a numerical study of (4.16); as we shall see, (5.16) gives us an extremely useful guide to the behaviour, nature, and existence of the various modes of instability present.

6. Solution of disturbance equation

6.1 Numerical method

For the purposes of numerical solution, equations (4.14) and (4.15) were chosen (in preference to (4.16)). A fairly straightforward Runge-Kutta scheme was applied to this system, with the shooting commencing at some suitably large value of η, with (4.19) and (4.20), and the computation proceding inwards, towards $\eta=0$. The impermeability condition at $\eta = 0$ was satisfied by choosing the appropriate value of c (by means of Newton's method).

In a number of computations it was found advantageous to divert the computation below the real η axis, in particular when $|w_0-c|$ was small (if $\mathrm{Im}(c) < 0$ this procedure must be used). A similar technique has been (used by Mack (1965), using a method based on that of Zaat (1958).

6.2 Doubly generalised inflexion point results

Before presenting details for the eigenvalue problem per se, defined in Section 4, we return briefly to consider further results for the basic flow. It was shown in Section 5 how the so called doubly generalised inflexion points are likely to play an important role in the stability of the flow. Consequently we return to consider the two examples studied in Section 3.2, namely $M_\infty = 2.8$ and $M_\infty = 3.8$. In particular we are interested in the existence of doubly generalised inflexion points.

Fig. 3a shows the axial variation of position of the doubly generalised inflexion points for $M_\infty = 2.8$. The point $\xi = 0$ corresponds to the leading edge of the cylinder, and as such corresponds to the planar case (as a result of our basic assumptions). There are two particularly striking features to this distribution: (i) that these points occur in pairs and (ii) there exists a critical value of ξ, downstream of which no such points exist. The upper

points are an extension of the generalised inflexion point found important in planar cases, whilst the lower points rise off the surface of the cylinder $\eta = 0$, to ultimately merge with the upper branch at $\xi \simeq 0.059$. It is remarkable how the doubly generalised inflexion points disappear at such a small distance downstream of the leading edge.

It was also shown in Section 5 how neutral solutions with wavespeed

$$c = w_0(\eta_i), \tag{6.1}$$

will occur, provided

$$1 - {}^1/_{M_\infty} < c < 1 + {}^1/_{M_\infty}, \tag{6.2}$$

and so in Fig. 3b we show the axial distribution of $w_0(\eta_i)$ for $M_\infty = 2.8$. Because of the restriction (6.2) it is seen that subsonic inflexional modes of instability will only occur for $0 < \xi \lesssim 0.047$, implying that such modes will completely disappear at just a distance approximately $0.0022 \times Re$ body radii downstream of the leading edge (although other modes types are certainly possible); consequently in this case we expect this mode will disappear before the doubly generalised inflexion points have merged. There are certain similarities here with the effect of cooling of planar boundary layers (Lees 1947, Mack 1987), which causes a similar effect on generalised inflexion points.

We next turn our attention to results for the higher Mach number considered previously, $M_\infty = 3.8$. Figure 3c shows the axial variation of the doubly generalised inflexion points in this case; the general characteristics are the same as those of Fig. 3a, except the range of ξ for which such points exist is increased. The corresponding distribution of $w_0(\eta_i)$ is shown in Fig. 3d; this too is similar to

the corresponding $M_\infty = 2.8$ distribution shown in Fig. 3b. In the case of $M_\infty = 3.8$, Fig. 3d indicates that neutral subsonic inflexional modes will disappear a distance approximately 0.013xRe body radii downstream of the leading edge.

Guided by the above observations, we now turn our attention to the eigenvalue problem for the two cases $M_\infty = 2.8$ and $M_\infty = 3.8$.

6.3 Growth rate results

Figure 4a shows the variation of c_i with α (where $c = c_r + i\, c_i$), for the case $M_\infty = 2.8$, at $\beta = 0$ (and hence corresponds to a planar example). The corresponding results for c_r are shown in Fig. 4b. Here, and in all results to follow, neutral points are denoted by a cross. These results (which are typical of previous planar results - see for example Mack 1987) show two distinct unstable modes. The first (to be referred to as mode I) originates as a sonic neutral disturbance (with $c_i = 0$, $c_r = 1 - 1/M_\infty$) at $\alpha = 0$, and terminates as a neutral inflexional subsonic mode at $\alpha \simeq 0.1$, where $c_r = w(\eta = \eta_i) \simeq 0.66$; this mode in fact continues, becoming a decaying mode, with $c_i < 0$, although we shall mainly concentrate our attention on growing/neutral modes).

The second mode (to be referred to as mode II) originates at $\alpha \simeq 0.4$ as a subsonic neutral mode with $c_i = 0$, $c_r = 1$ (this may be regarded as a special case of an inflexional mode, with the generalised inflexion point occuring in the freestream). This mode then terminates at $\alpha \simeq 1.13$ as a (second) neutral subsonic inflexional instability (and at values of α greater than this value continues as a decaying mode, with $c_i < 0$).

Although other modes of instability undoubtedly exist at this Mach number, these have considerably smaller growth rates than modes I and II shown here, and are subsequently much less important from a practical

point of view. Note that since the (temporal) growth rate is αc_i, mode II is the most important.

We now turn to results incorporating the effects of curvature. Fig. 4c and Fig. 4d show distributions of c_r and c_i (respectively), with α (for $M_\infty = 2.8$), at $\delta = 0.02$. Although the qualitative features resemble those of the $\delta = 0$ case, the maximum amplitude of the growth rates is seen to be considerably reduced (in spite of the smallness of δ), particularly that of mode I.

Moving further down the axis of the cylinder, to $\delta = 0.04$, Figs. 4e (c_i distribution) and 4f (c_r distribution) indicate that mode I has practically disappeared, whilst the maximum amplitude of mode II is now significantly diminished, terminating (at a subsonic inflexional neutral point) at quite a large value of α ($\simeq 2.65$), although over much of the range of α, this mode has exceedingly small growth rates.

Following our comments in the previous subsection regarding $w_0(\eta_i)$ dropping below $1-1/M_\infty$, we expect mode I to completely disappear at $\delta \simeq 0.047$ for this choice of M_∞. As a consequence, the next set of results (at $\delta = 0.05$) presented in Fig. 4g (c_i) and Fig. 4h (c_r) shows just mode II, which itself exhibits a further reduction in growth rate. This mode still originates as a neutral mode with $c_r = 1$ (at $\alpha \simeq .45$); unfortunately our computations did not indicate a clear neutral solution at an upper value of α. This was due to the exceedingly small growth rates encountered, which were typically $0(10^{-10})$, and hence were comparable with the round-off associated with the computation. (In the regime of larger α and very small growth rates, it was found to be most essential to deform the integration contour in the numerical scheme, as described in Section (6.1), in order to maintain

numerical accuracy.) If a neutral point exists, as seems likely, it must be of the neutral supersonic class ($c_i = 0$, $c_r < 1 - 1/M_\infty$) because of the absence of any doubly generalised inflexion points at this value of ζ.

As a final example of the $M_\infty = 2.8$ flow, we show results for $\zeta = 0.2$ in Figs. 4i (c_i) and 4j (c_r). These indicate qualitative similarity with the previous set of results; however the maximum growth rate is reduced by approximately an order of magnitude. Again, unfortunately, positive identification of an upper neutral point was not possible, due to the difficulties with tiny growth rates encountered at larger values of α. We conclude, however , that curvature has important (and profound) effects: (i) annihilation of mode I and (ii) substantial reduction of the growth rate of mode II (although the range of α over which this unstable mode exists is increased quite significantly).

We next turn our attention to results for $M_\infty = 3.8$, and Figs. 5a and 5b show c_i and c_r distributions (respectively) with α, for the particular case $\zeta=0$. This corresponds to the planar case as computed previously (Mack 1987 for example) and thus provides a useful check on the accuracy of the present overall scheme, (which is seen to be entirely satisfactory). When compared with the corresponding $M_\infty = 2.8$ results (Figs. 4a, 4b), the importance of mode II is seen to be significantly increased (although the growth rate of mode I is increased also). Generally, the $M_\infty = 3.8$ distributions qualitively resemble the corresponding $M_\infty = 2.8$ distributions.

At $\zeta = 0.05$ (with $M_\infty = 3.8$), we see in Figs. 5c (c_i distribution) and 5d (c_r distribution) there is an approximate halving of the maximum growth rate, when compared with the $\zeta=0$ results. Further

downstream, at $\zeta = 0.10$ (Figs. 5e, 5f) mode I has almost disappeared, whilst mode II has suffered a further depletion of maximum growth rate.

From our observations made in Section (6.2), we expect that mode I will completely disappear at $\zeta \simeq 0.013$ (where $c_r = w_0(\eta - \eta_i) = 1 - 1/M_\infty$); this will also be an important location for the upper neutral point of mode II, which for $\zeta < 0.013$ is of the subsonic inflexional kind. As noted earlier, for the previous M_∞ considered, growth rates in this regime were extremely small, and so no firm conclusions on the behaviour of this mode in this region were possible. Fortunately, although the growth rates in this critical region at $M_\infty = 3.8$ are small, they are nonetheless significantly larger than at the lower Mach number.

Figure 5g shows the <u>local</u> variation of c_i with α at $\zeta = 0.112$ (just below the critical value). Mode II is clearly seen to become a damped mode at $\alpha \simeq 0.85$, with $|c_i|$ reaching a maximum at $\alpha \simeq 0.93$, and then decreases. Unfortunately, no firm conclusions are possible regarding the ultimate behaviour of c_i at large values of α, due to the smallness of $|c_i|$.

Figure 5h shows the distribution of c_i in the same critical region of α, at $\zeta = 0.114$ (slightly above the critical value of ζ). It now appears that the growing mode II now terminates at $\alpha \simeq 0.94$, as a supersonic neutral mode, <u>and does not continue as a damped mode</u>. Instead, a further (supersonic) neutral mode has already appeared (at $\alpha \simeq 0.88$) and this is then the origin of a damped mode, which has a maximum value of $|c_i|$ at $\alpha \simeq 0.95$; $|c_i|$ then decreases, towards zero, and again because of its ultimate smallness, no conclusions regarding its behaviour at larger values of α are possible.

Additionally, there was some evidence of another unstable mode, beginning around $\alpha \simeq 1.52$, but because of its very small growth rate it is not possible to be completely categorical about this; its growth rate was also too small to be seen on the scale of Fig. 5h. Thus in this case we see the presence of possibly three (supersonic) neutral points in this regime.

Figure 5i details the variation of c_i in the crucial α region, for the location $\bar{y} = 0.116$. Again, (growing) mode II is seen to terminate at a supersonic neutral point, this time located at $\alpha \simeq 1$. A further supersonic neutral point exists, originating at $\alpha \simeq 0.9$ which then provides the start for a decaying mode; when compared to the corresponding $\bar{y} = 0.114$ mode, the decay rate of this particular mode is seen to be reduced. Further, this mode now seems to terminate at another neutral point (at $\alpha \simeq 1.48$). Yet another neutral point exists at $\alpha \simeq 1.40$, which then provides the start of a second unstable mode (although the growth rate of this mode was so small to be bearly visible on Fig. 5i); a total of four supersonic neutral points are thus observed in this region of α.

Figure 5j shows the c_i distribution at $\bar{y} = 0.118$ in the same general region of α. When compared with the previous results, a further change to the qualitative picture is seen. Here, the original mode II has merged with the second unstable mode. Just two neutral points remain in this region, at $\alpha \simeq 0.93$ and $\alpha \simeq 1.35$, which are associated with the start and the terminus of the decaying mode (which generally has a significantly reduced $|c_i|$ compared to the previous results). The ultimate behaviour of the growing mode with α remains unclear, due to the smallness of $|c_i|$.

It is interesting to note that when two modes were present (for a given value of α), both modes had values of c_r that were practically indistinguishable. Further, there was no difficulty in

calculating accurate values of c_r, even at large values of α.

Moving further downstream to $\xi = 0.2$, the decaying mode has disappeared completely, and c_i and c_r distributions over a broad range of α are shown in Figs. 5k and 5ℓ respectively. When compared with the Fig. 5e results, the mode II growth rates are quite appreciably reduced; the ultimate behaviour of $|c_i|$ at large values of α remains unclear.

Further downstream still, at $\xi = 1.0$, results (c_i shown in Fig. 5m, c_r shown in Fig. 5n) are qualitively similar to those at $\xi = 0.2$, except that the maximum value of c_i is significantly diminished, and occurs at a rather larger value of α (as does the origin of this mode which occurs at $\alpha \simeq 0.72$, compared with $\alpha \simeq 0.4$ in the case of $\xi = 0.2$). The larger α behaviour of this mode is again unclear, due to the reasons described above.

In the following section we turn to consider a number of general conclusions and points raised by this work.

7. Conclusions

In this paper the supersonic flow over a thin straight circular cylinder has been investigated. The basic boundary layer flow has been obtained, and the inviscid stability of the flow has been studied. A condition on the basic flow for the existence of so called subsonic inflexional neutral modes of instability has been derived, and is found to be an extension of the generalised inflexional condition relevant to planar flows.

The effect of body surface curvature is seen to immediately (and significantly) reduce the importance of the "first mode" of inviscid instability, which is seen to completely disappear at what could be a comparatively short distance down the axis of the cylinder (by about 0.0022 x Re body radii at $M_\infty = 2.8$, and by about 0.013xRe body radii at $M_\infty = 3.8$).

The maximum growth rate of the "second mode" of inviscid instability also suffers a substantial reduction at locations increasingly further down the axis of the cylinder, although the evidence is that it does not disappear completely.

There are certain similarities here with the effect of cooling a planar boundary layer (Mack 1984, 1987, for exmaple), which can also cause the first mode to disappear completely (cooling also causes the formation of a second generalised inflexion point, which with a progressive reduction in wall temperature eventually coalesces with the first generalised inflexion point). However the effect of cooling is to increase the amplification rate of the second mode (in contrast to our results featuring curvature).

It is particularly interesting to note that although inviscid modes of instability are generally regarded as more important/ unstable than viscous modes of instability in the case of supersonic

planar flows, the work of Duck and Hall (1988a,b) on viscous axisymmetric flows indicates that a reduction in body radius (equivalent to a further downstream location in our context) causes an increase in amplification rate. Thus it is entirely possible that with axisymmetric flows, regimes may exist where viscous instability is dominant.

It is to be hoped that this study will provide a basis for the study of flows over further and more practical geometries, such as cones. One important omission to the physics of that problem, which must ultimately be resolved, is the exclusion of any shock waves in the basic flow (however this may be justified by the restriction of thinness), although previous works on planar flows (cited throughout this paper) all have this same omission. It is also hoped that these results will provide material for comparison with finite Reynolds number computations.

Acknowledgements

This research was supported by the National Aeronautics and Space administration under NASA contracts No. NAS1-18605 and NAS1-18107 while the author was in residence at the Institute for Computer Applications in Science and Engineering (ICASE), NASA Langley Research Center, Hampton, VA 23665.

The author wishes to thank Mr. Stephen Shaw (University of Manchester) for a number of useful comments on this work. A number of computations were carried out at the University of Manchester Computer Centre with computer time provided under S.E.R.C. Grant number GR/E/25702.

REFERENCES

Brown, W.B. 1962 Exact numerical solutions of the complete linearized equations for the stability of compressible boundary layers. Norair Report No. NOR-62-15 Northrup Aircraft Inc., Hawthorne, CA.

Bush, W.B. 1976 Axial incompressible viscous flow past a slender body of revolution. Rocky Mountain J. of Math. 6, 527.

Duck, P.W. and Bodonyi, R.J. 1986 The wall jet on an axisymmetric body. Quart. J. Mech. Appl. Maths. 39, 407.

Duck, P.W. and Hall, P. 1988a On the interaction of axisymmetric Tollmien-Schlichting waves in supersonic flow. ICASE report no. 88-10 (to appear in Quart. J. Mech. Appl. Maths).

Duck, P.W. and Hall, P. 1988b Non-axisymmetric viscous lower branch modes in axisymmetric supersonic flows. ICASE report no. 88-42 (submited to J.Fluid.Mech).

Glauert, M.B. and Lighthill, M.J. 1955 The axisymmetric boundary layer on a long thin cylinder. Proc. R. Soc. Lond. A230, 188.

Küchemann, D. 1938 Störungsbewegunyen in einer Gasströmung mit Grentschicht, ZAMM 18, 207.

Lees, L. 1947 The stability of the laminar boundary layer in a compressible fluid. NACA Tech. report No. 876.

Lees, L. and Lin, C.C. 1946 Investigation of the stability of the laminar boundary layer in a compressible fluid. NACA Tech. Note No. 1115.

Lin, C.C. 1945 On the stability of two-dimensional parallel flows, parts I, II, III, Quart. Appl. Math., 3, 117, 218, 277.

Mack, L.M. 1963 The inviscid stability of the compressible laminar boundary layer, in "Space programs summary", no. 37-23, p. 297. JPL, Pasadena CA.

Mack, L.M. 1964 The inviscid stability of the compressible laminar boundary layer: Part II, in "Space programs summary", No. 37-26, Vol IV p165, JPL Pasadena, CA.

Mack, L.M. 1965a. Stability of the compressible laminar boundary layer according to a direct numerical solution, in AGARDograph 97, part I, 329.

Mack, L.M. 1965b Computation of the stability of the laminar boundary layer, in "Methods in computational physics". (B. Alder, S. Fernbach and M. Rotenberg eds). vol 4, 247, Academic, N.Y.

Mack, L.M. 1969 Boundary-layer stability theory, JPL, Pasadena, CA, Document No. 900-277, Rev. A.

Mack, L.M. 1984, Boundary-layer linear stability theory in "Special course on stability and transition of laminar flow", AGARD Report No. 709, 3-1.

Mack, L.M. 1987 Review of compressible stability theory in Proc. ICASE workshop on the stability of time dependent and spatially varying flows, Springer-Verlag.

Moore, F.K. 1955 Unsteady laminar boundary layer flow. NACA. Tech. Note 2471.

Reshotko, E. 1962 Stability of Three-dimensional compressible boundary layers. NASA Tech. Note D-1220.

Seban, R.A. and Bond, R. 1951 Skin friction and heat transfer characteristics of a laminar boundary layer on a cylinder in axial incompressible flow. J. Sci. 10, 671.

Stewartson, K. 1951 On the impulsive motion of a flat plate in a viscous fluid. Quart. J. Mech. Appl. Maths. 4, 182.

Stewartson, K. 1955 The asymptotic boundary layer on a circular cylinder in axial incompressible flow. Quart. appl. Math. 13, 113.

Stewartson, K. 1964 The theory of laminar boundary layers in compressible fluids. Oxford University Press.

Thompson, P.A. 1972 Compressible fluid dynamics. Mc. Graw-Hill.

Zaat, J.A. 1958 Numerische Beiträge zur Stabilitätstheorie de Grenzschichten, Grenzschichtforschung Symp., IUTAM 127, Springer, Berlin.

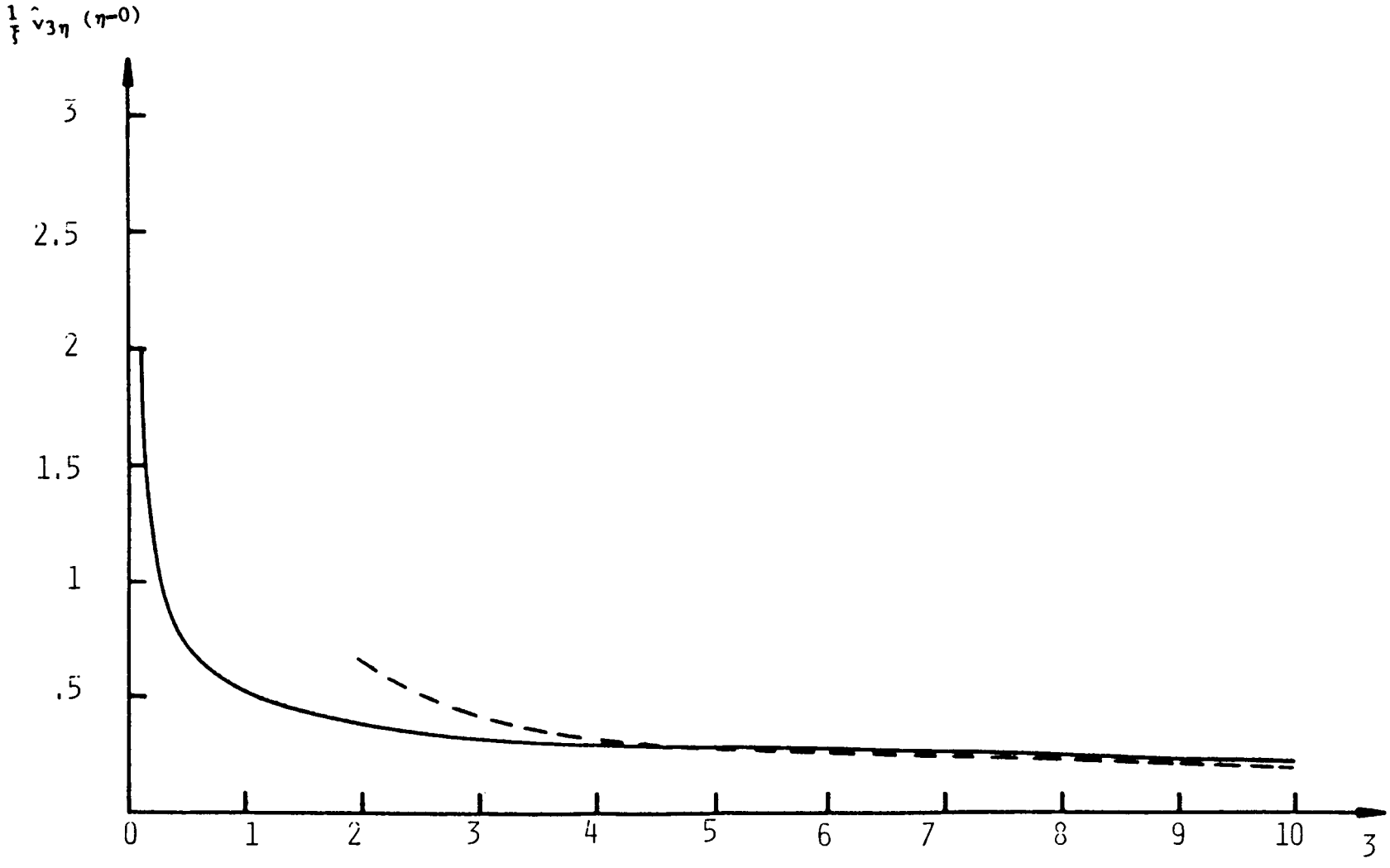

Fig 1a Variation of $\frac{1}{\xi}\hat{v}_{3\eta}(\eta=0)$ with ξ, $M_\infty = 2.8$.

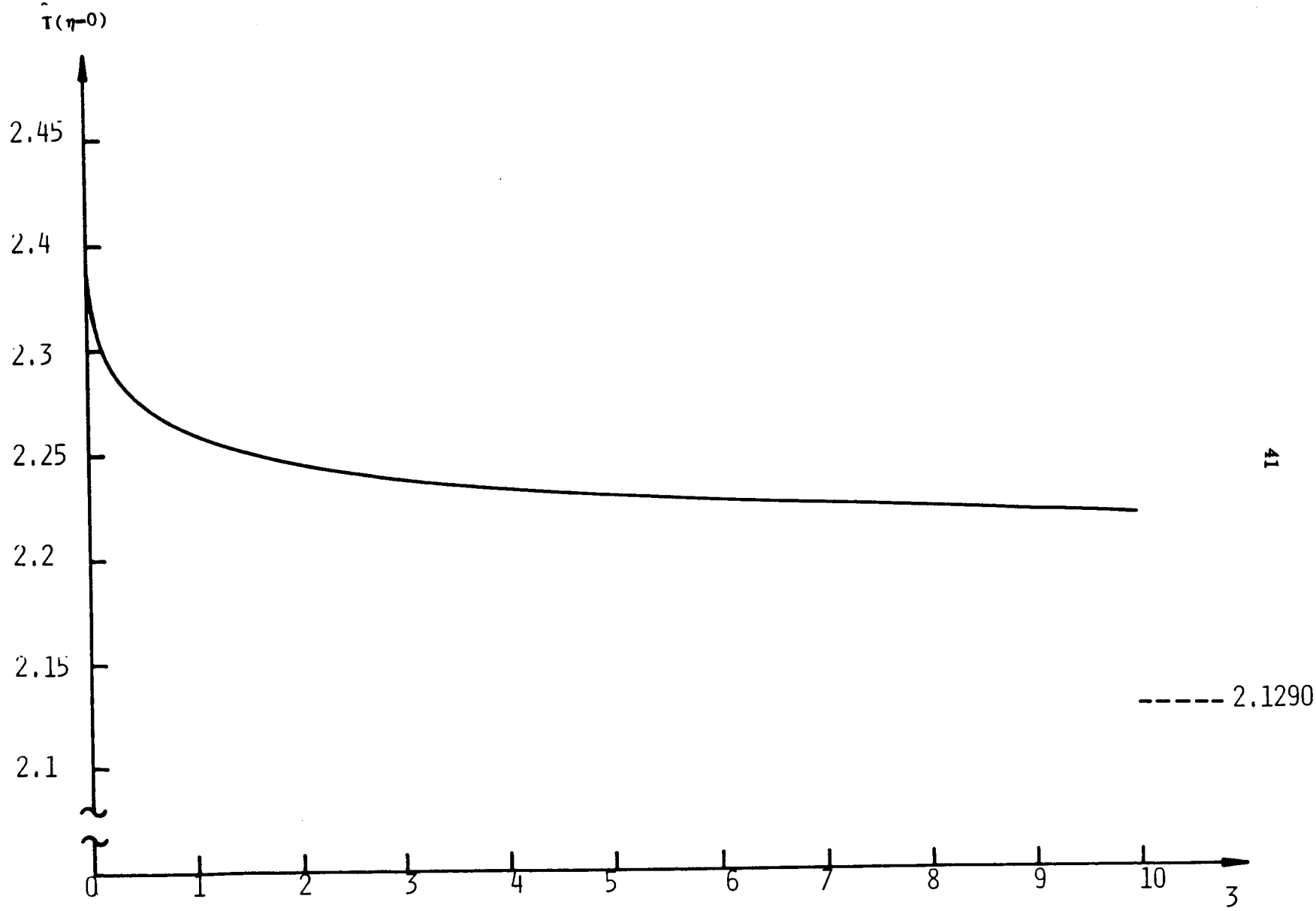

Fig 1b Variation of $\hat{T}(\eta=0)$ with ζ, $M_\infty = 2.8$.

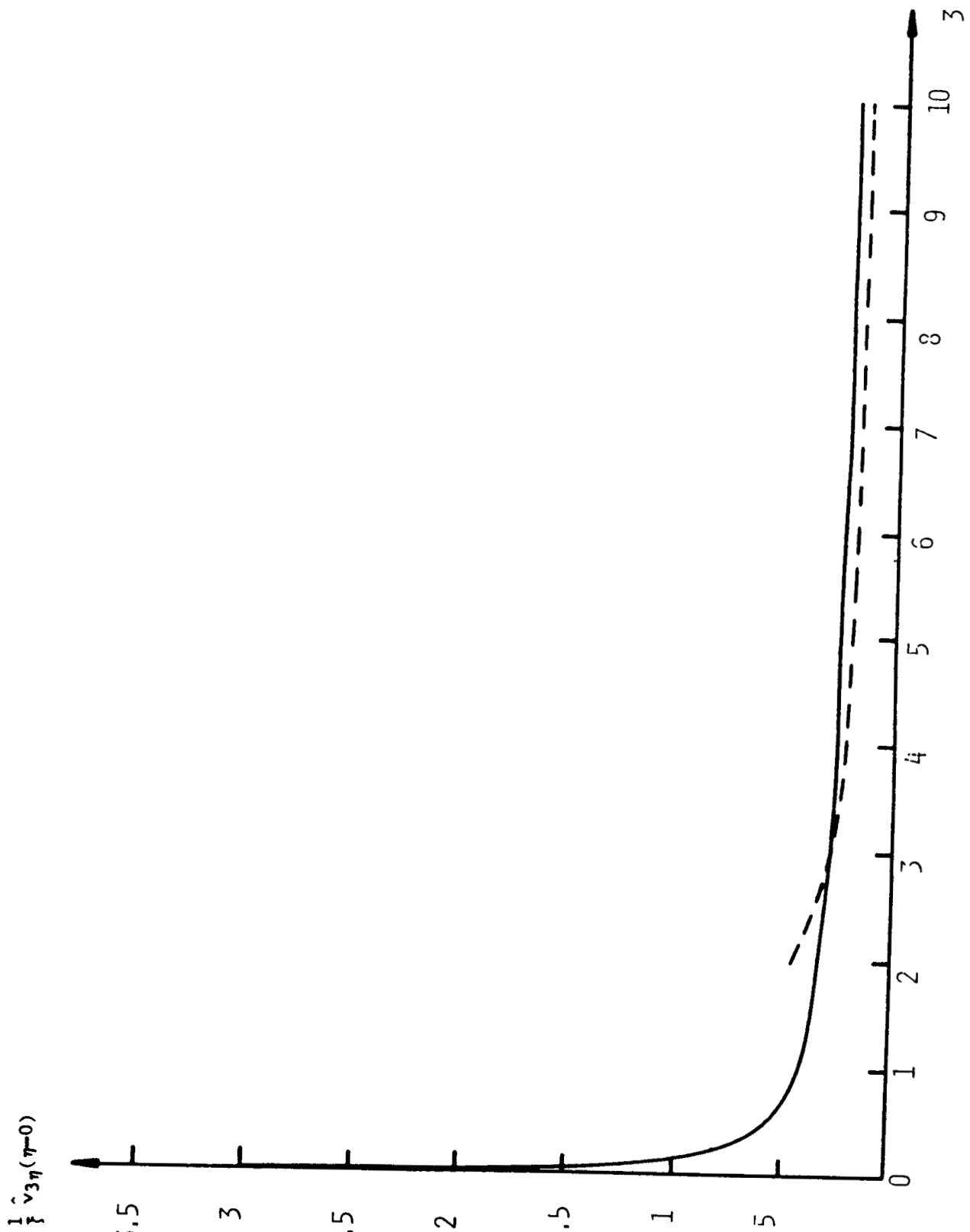

Fig 2a Variation of $\frac{1}{\xi}\hat{v}_{3\eta}$ $(\eta=0)$ with ξ, $M_\infty = 3.8$.

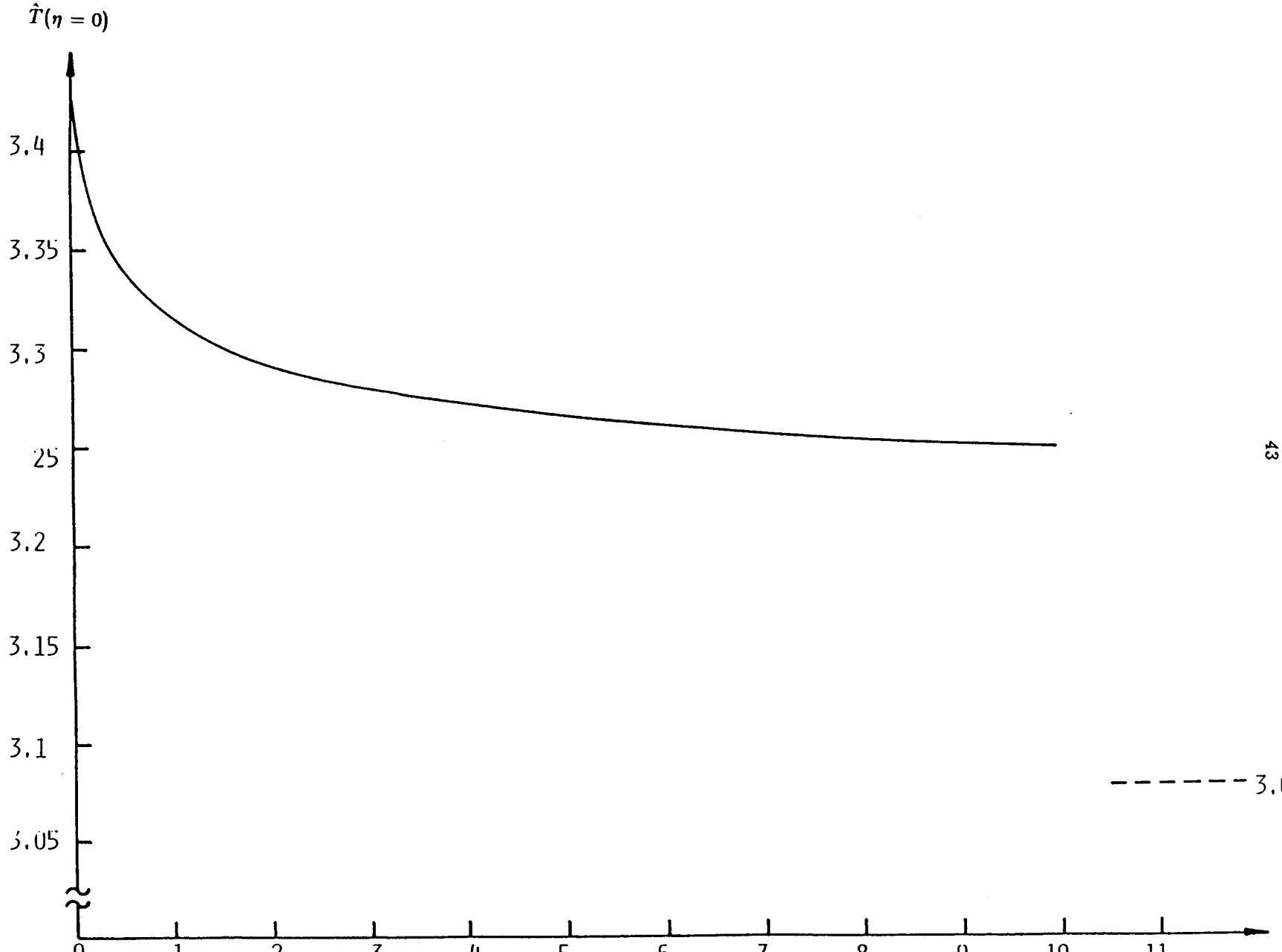

Fig 2b Variation of $\hat{T}(\eta=0)$ with ξ, $M_\infty = 3.8$

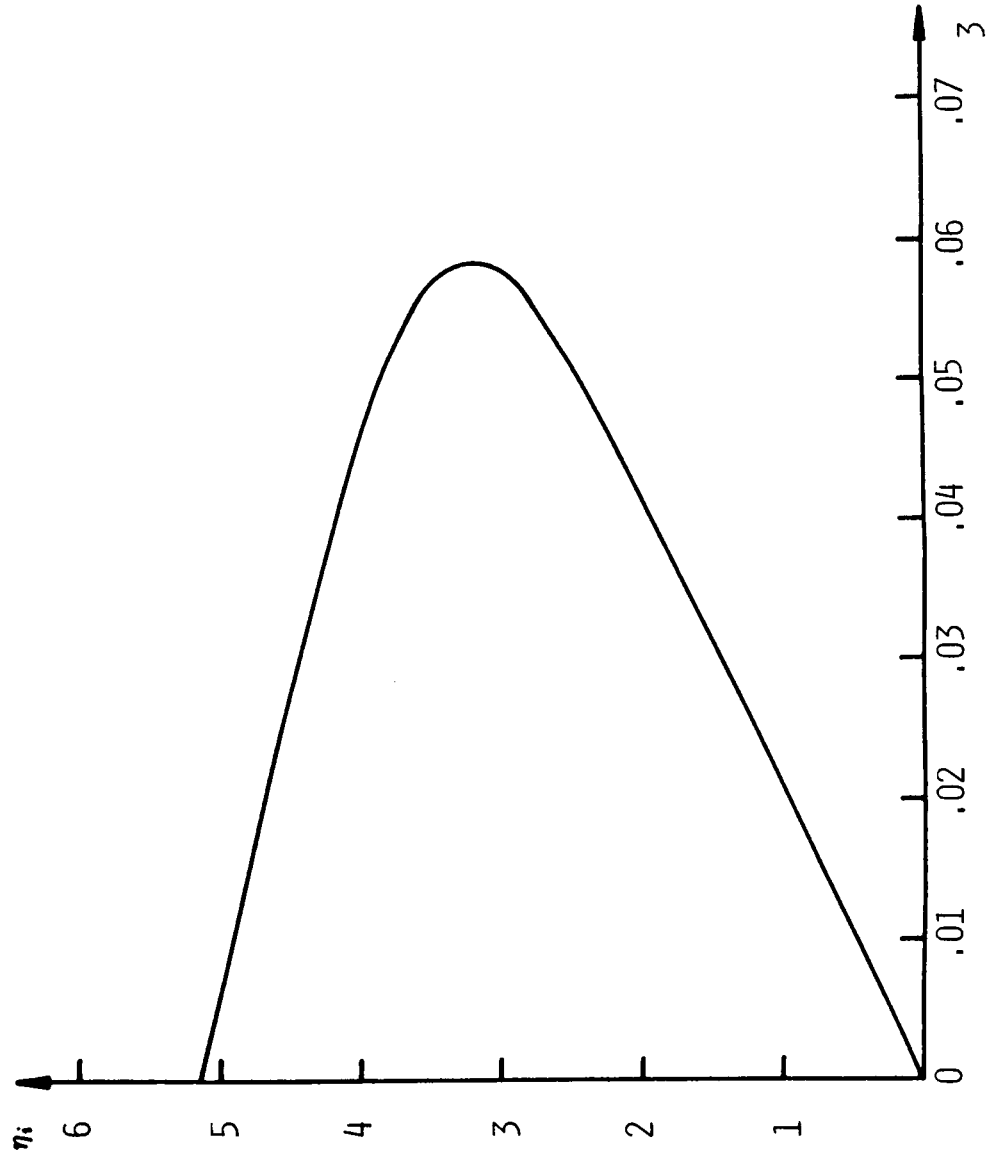

Fig 3a Variation of transverse positions of inflexion points (η_i)

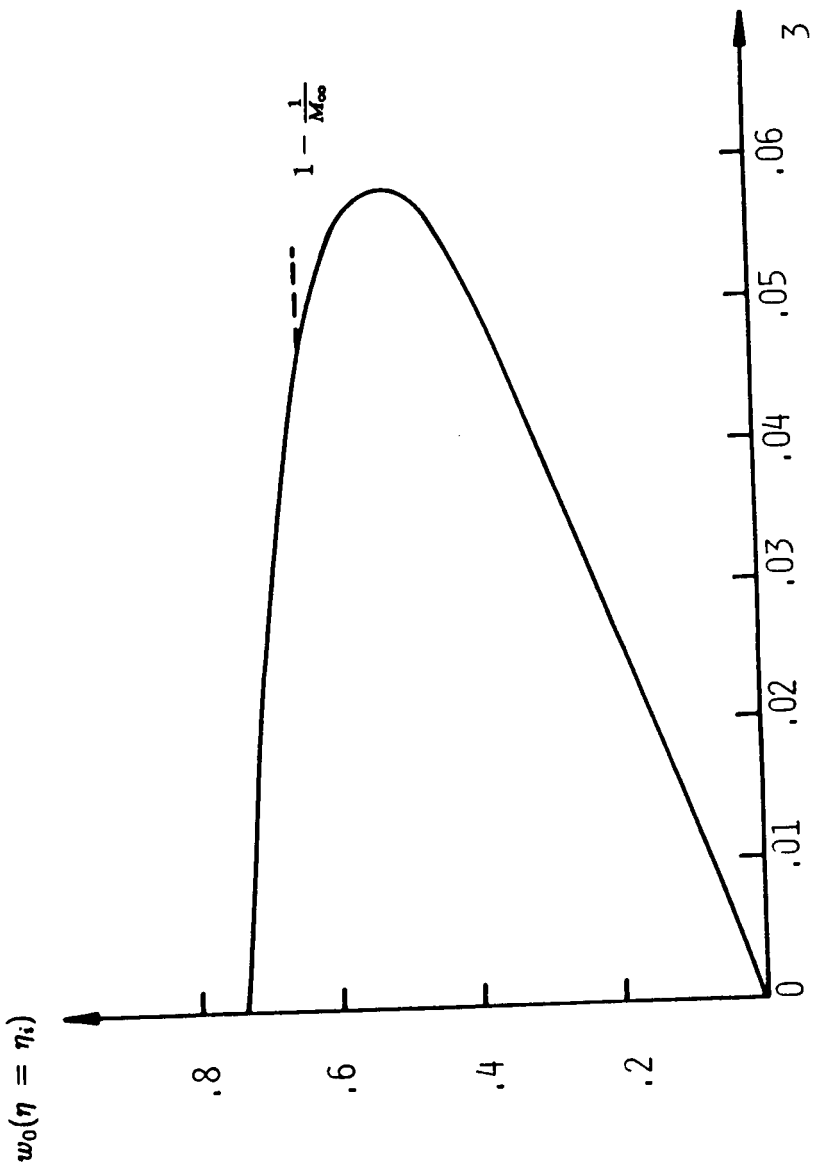

Fig 3b Variation of $w_0(\eta-\eta_i)$ with ζ, $M_\infty = 2.8$.

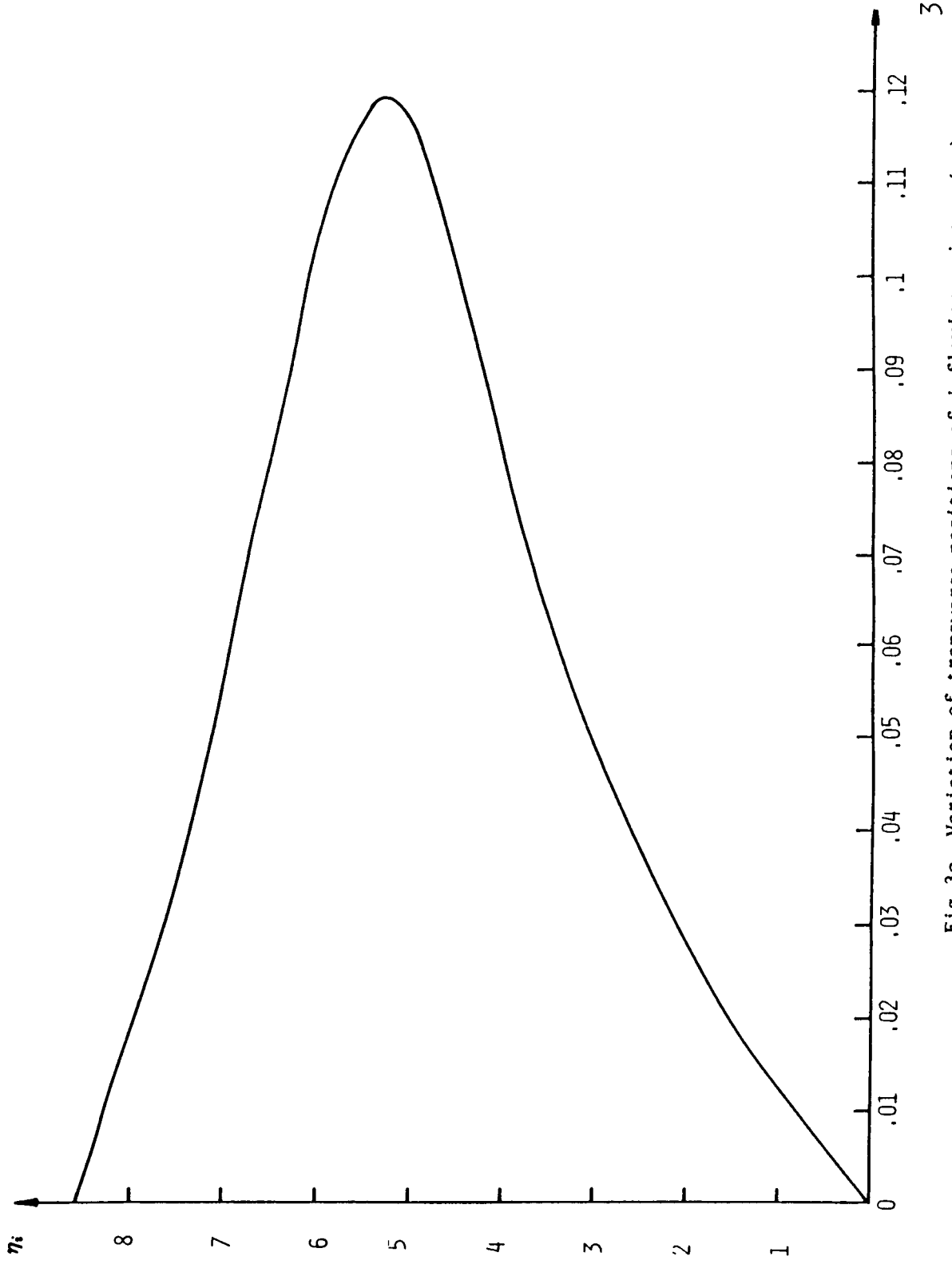

Fig 3c Variation of transverse positions of inflexion points (η_i) with axial location (ξ), $M_\infty = 3.8$.

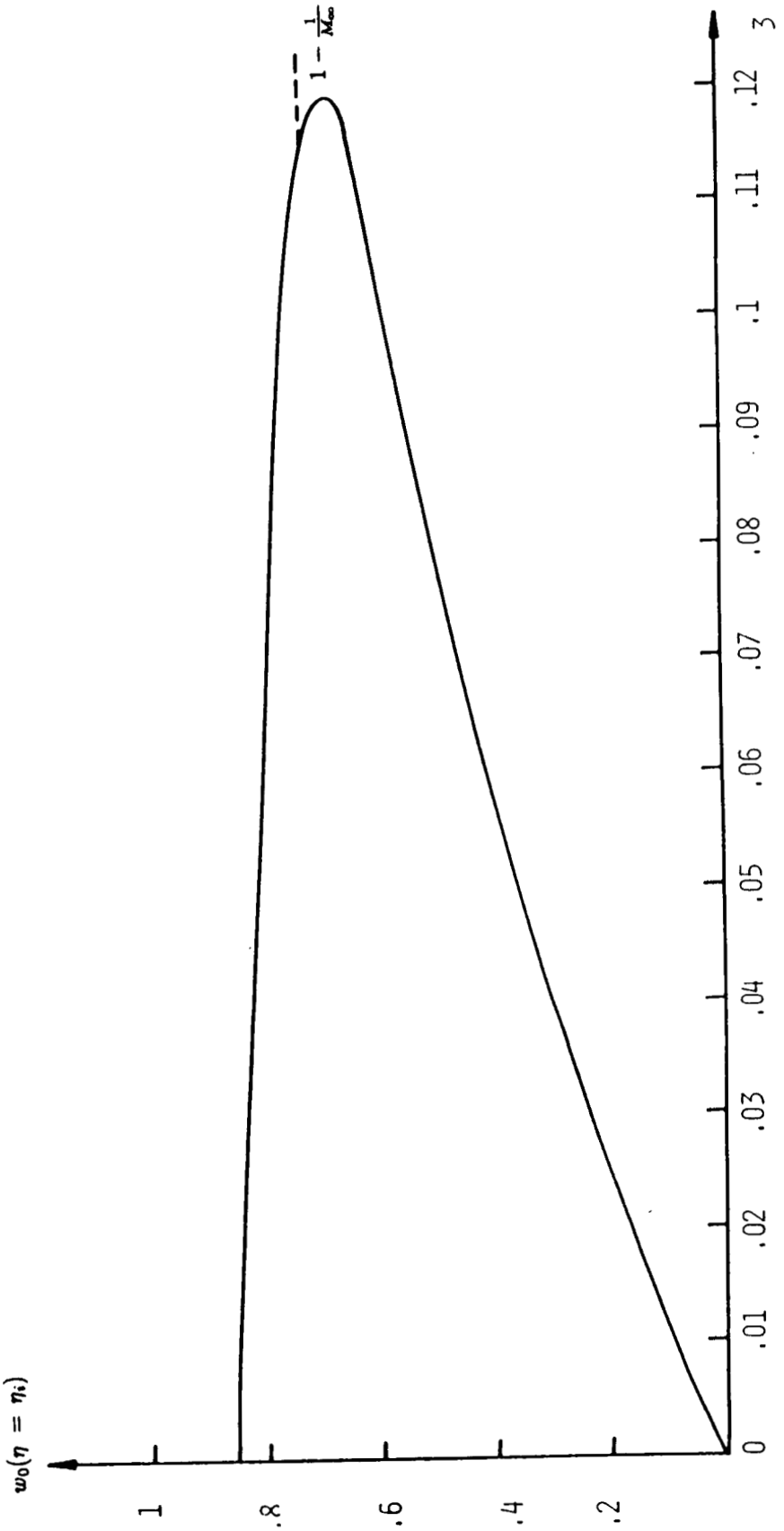

Fig 3d Variation of $w_0(\eta=\eta_i)$ with ζ, $M_\infty = 3.8$

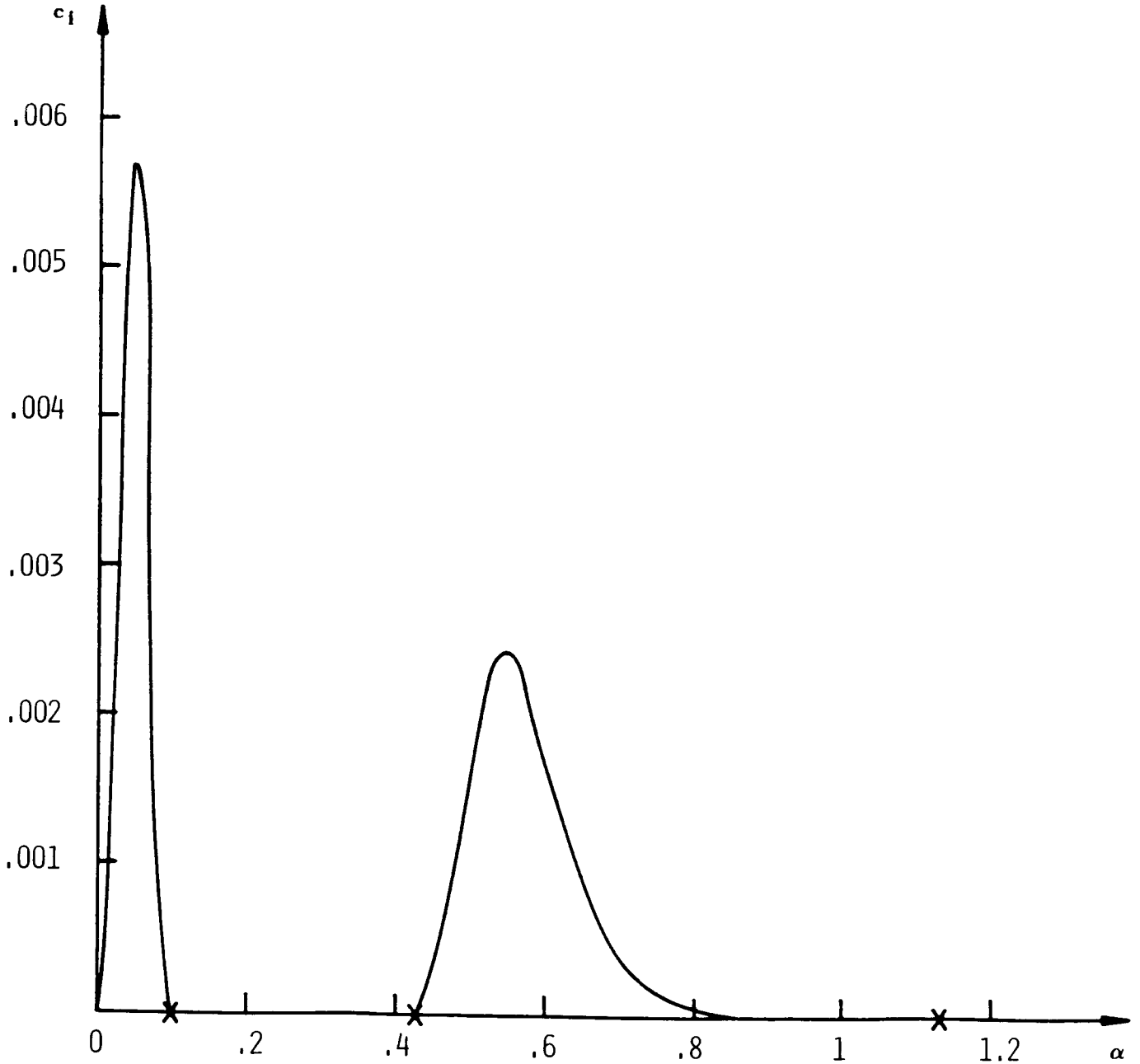

Fig 4a Variation of c_i with α, $M_\infty = 2.8$, $\gamma = 0$ (planar case)

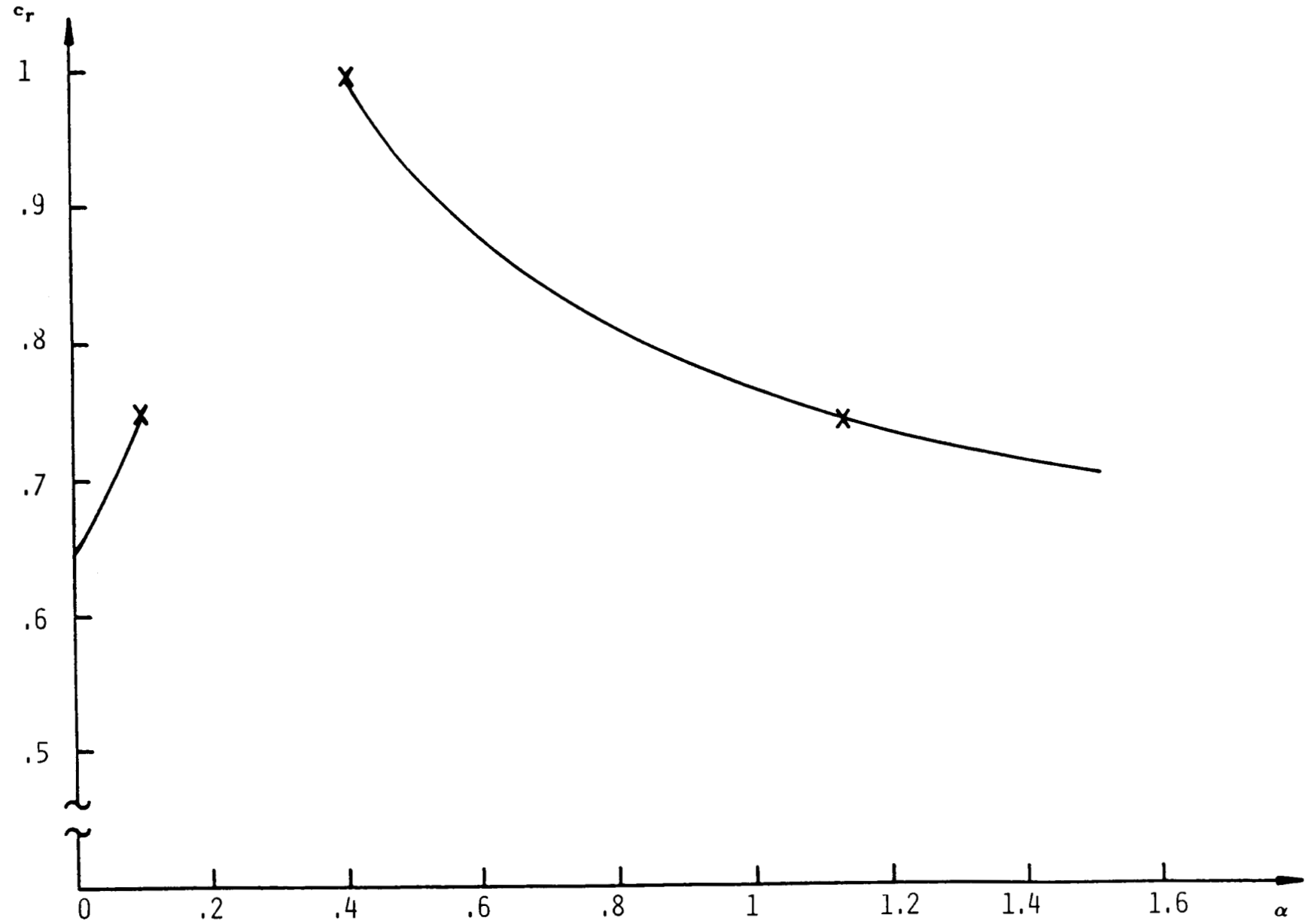

Fig 4b Variation of c_r with α, $M_\infty = 2.8$, $\gamma = 0$ (planar case)

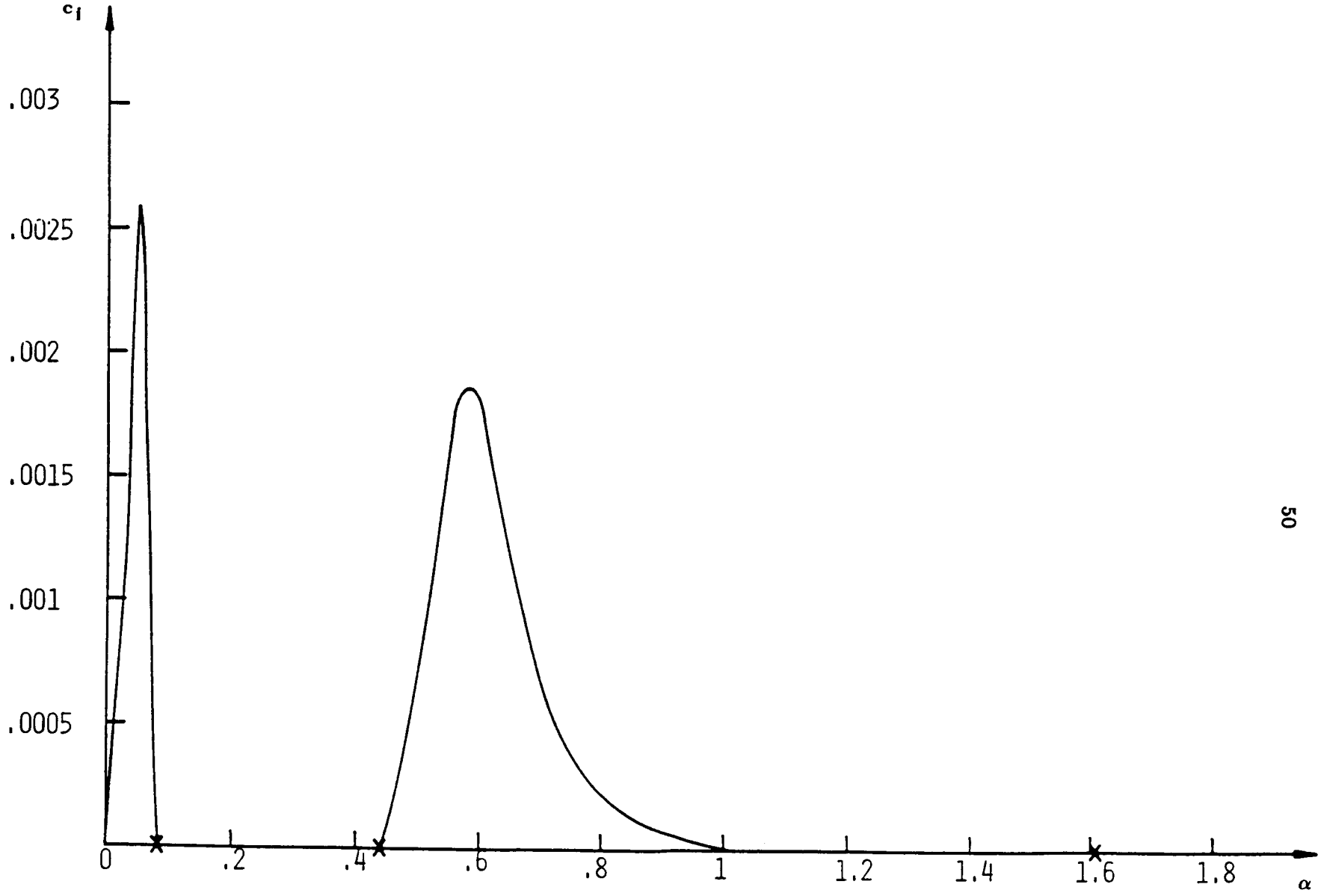

Fig 4c Variation of c_i with α, $M_\infty = 2.8$, $\varsigma = 0.02$

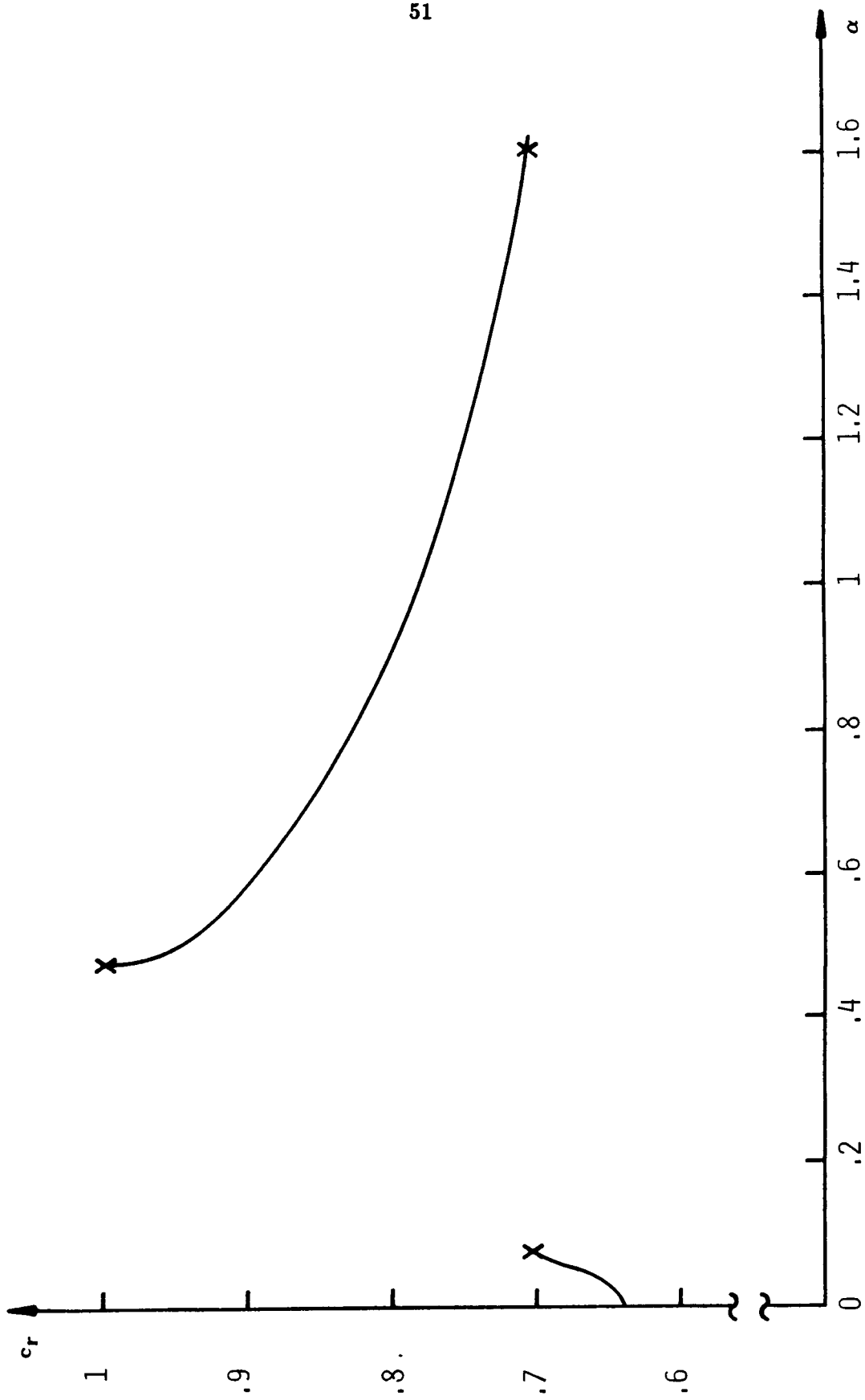

Fig 4d Variation of c_r with α, $M_\infty = 2.8$, $\gamma = 0.02$

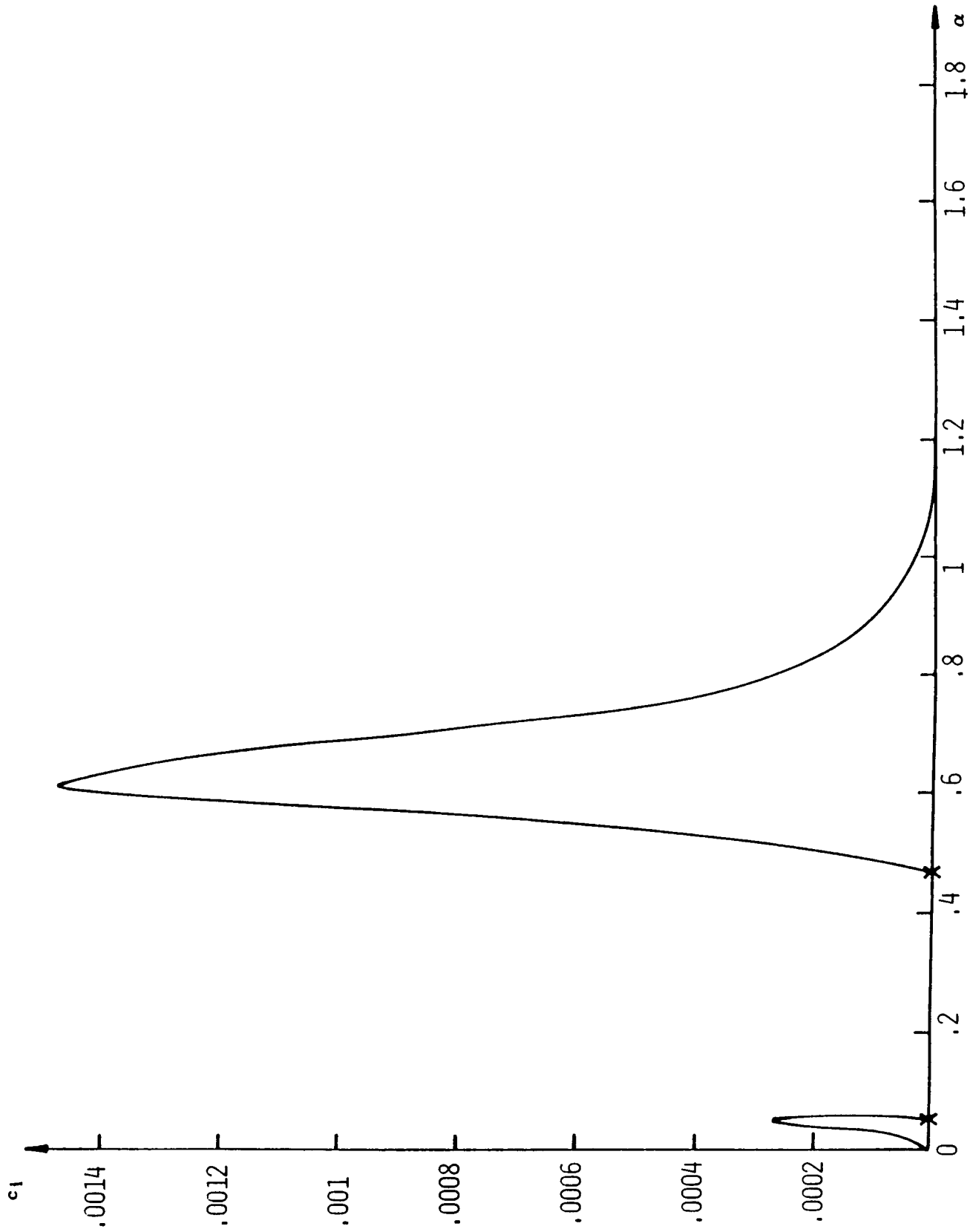

Fig 4e Variation of c_i with α, $M_\infty = 2.8$, $\tau = 0.04$

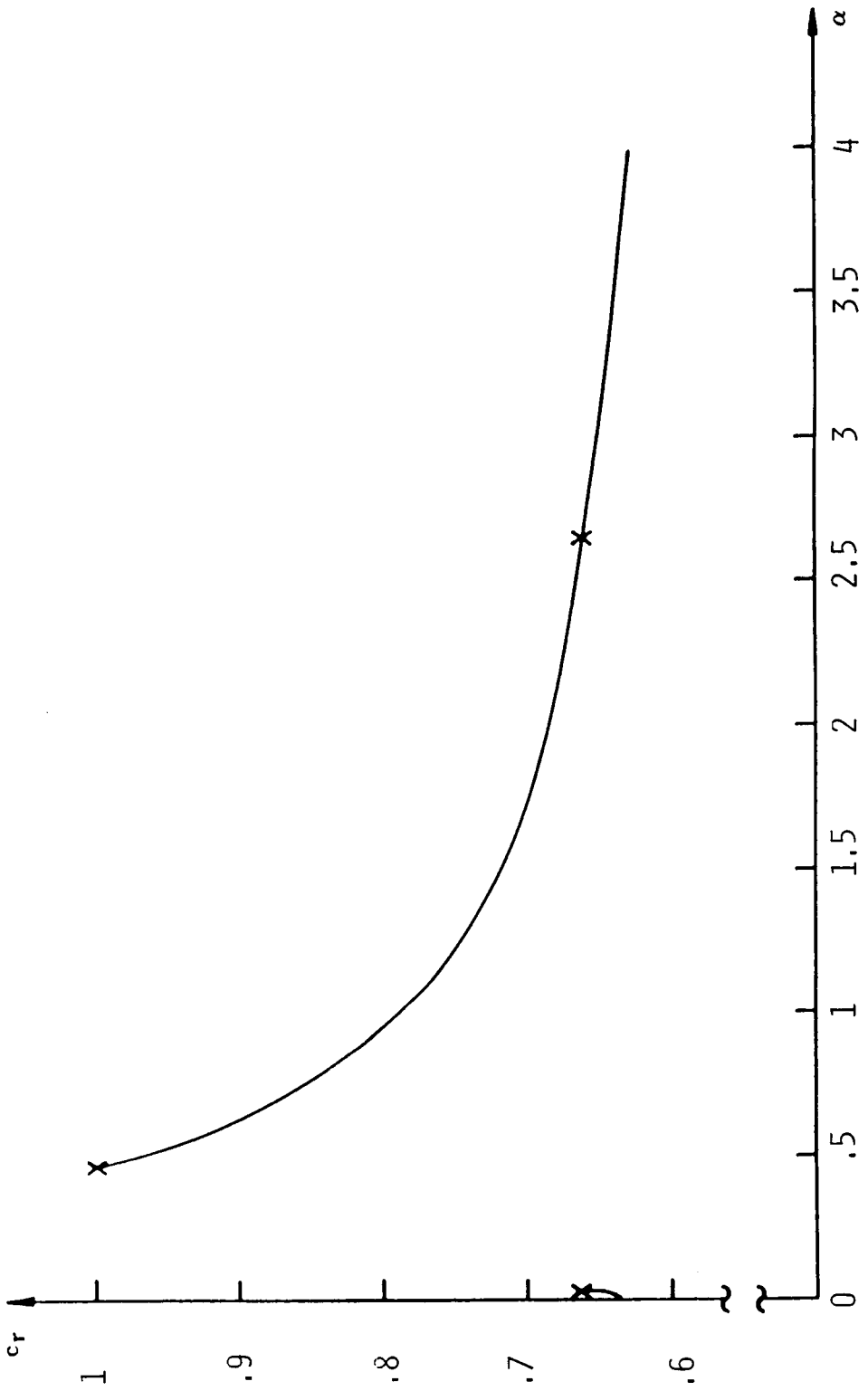

Fig 4f Variation of c_r with α, $M_\infty = 2.8$, $\zeta = 0.04$

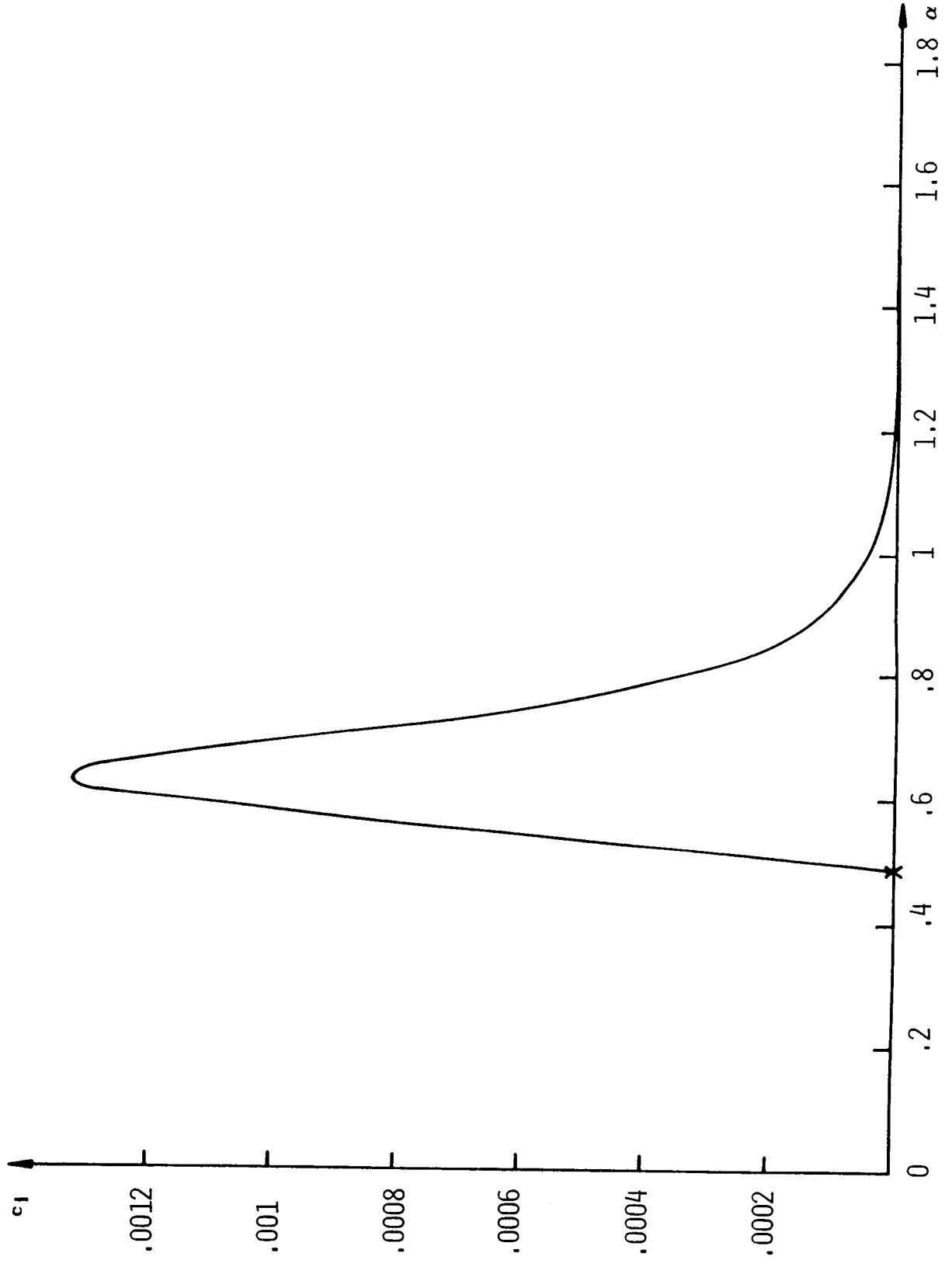

Fig 4g Variation of c_l with α, $M_\infty = 2.8$, $t = 0.05$

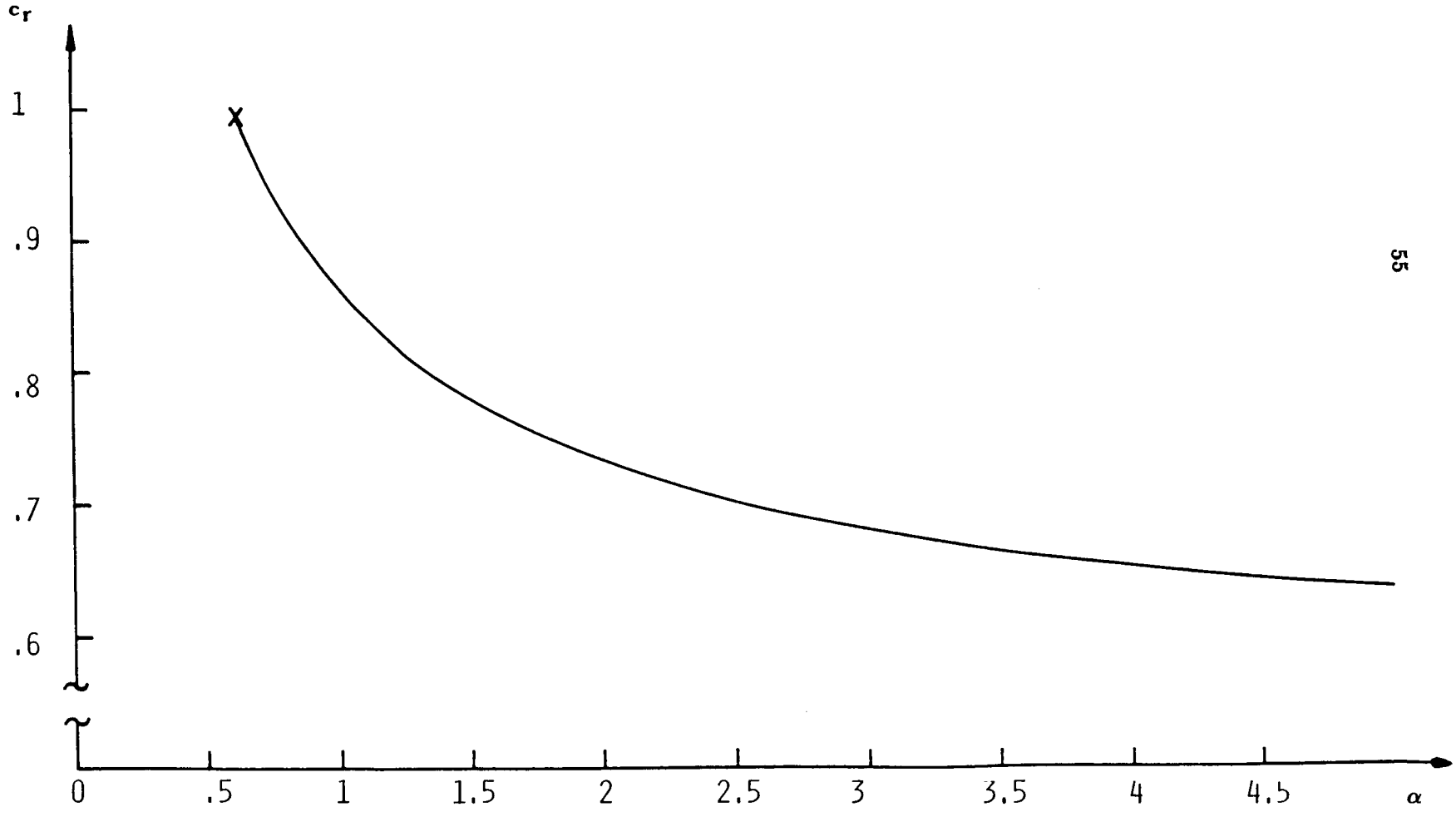

Fig 4h Variation of c_r with α, $M_\infty = 2.8$, $\delta = 0.05$

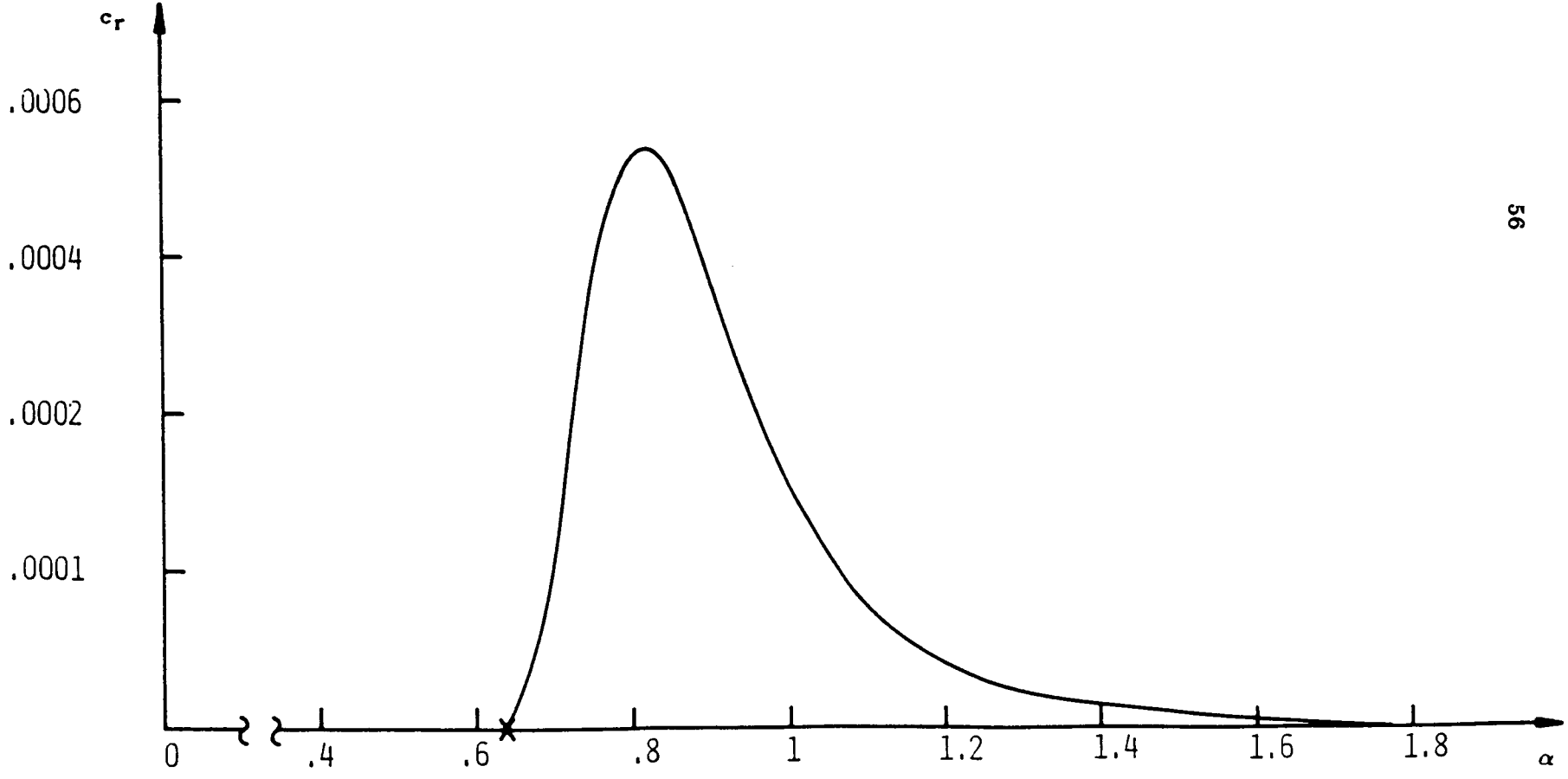

Fig 4i Variation of c_i with α, $M_\infty = 2.8$, $\zeta = 0.2$

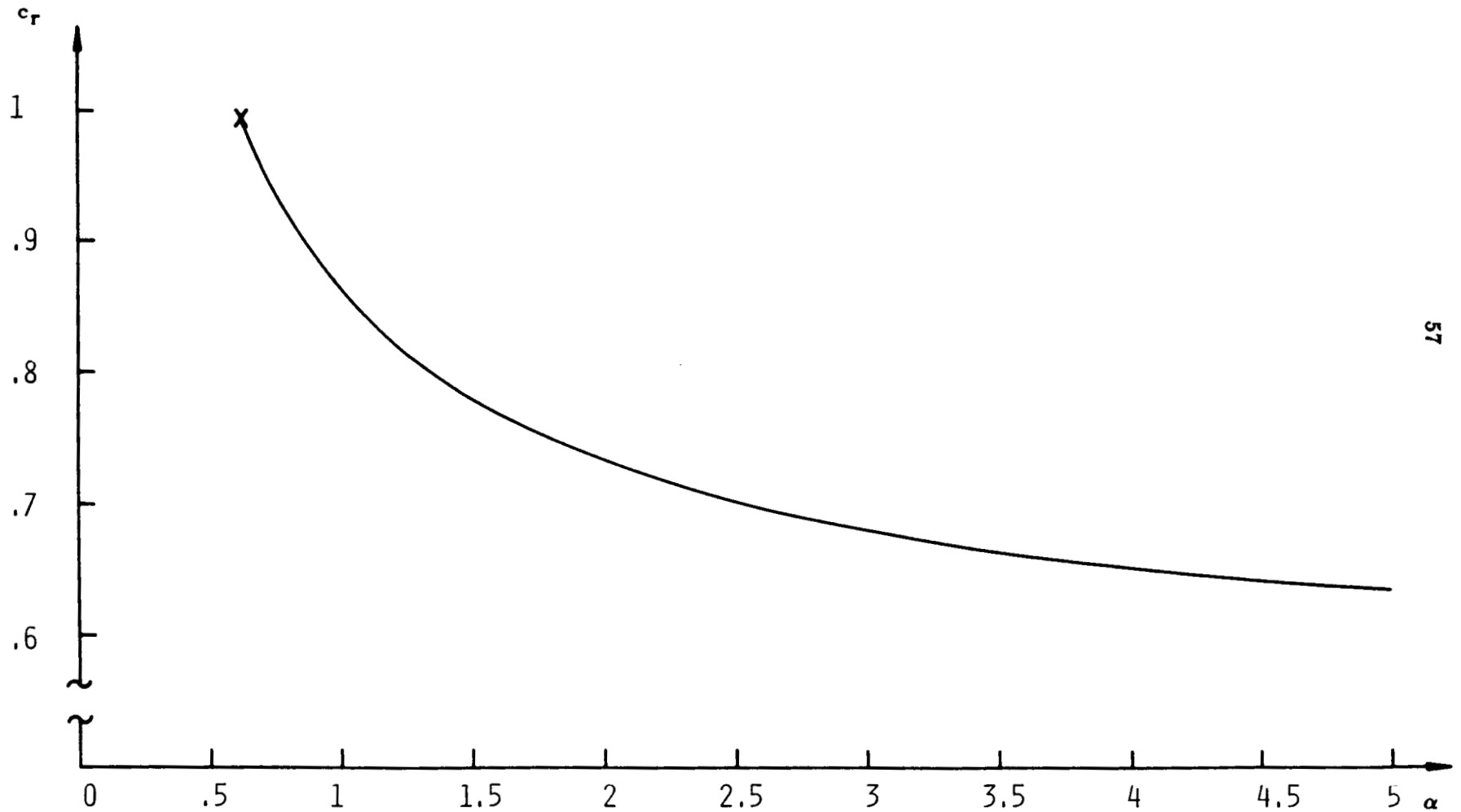

Fig 4j Variation of c_r with α, $M_\infty = 2.8$, $\zeta = 0.2$

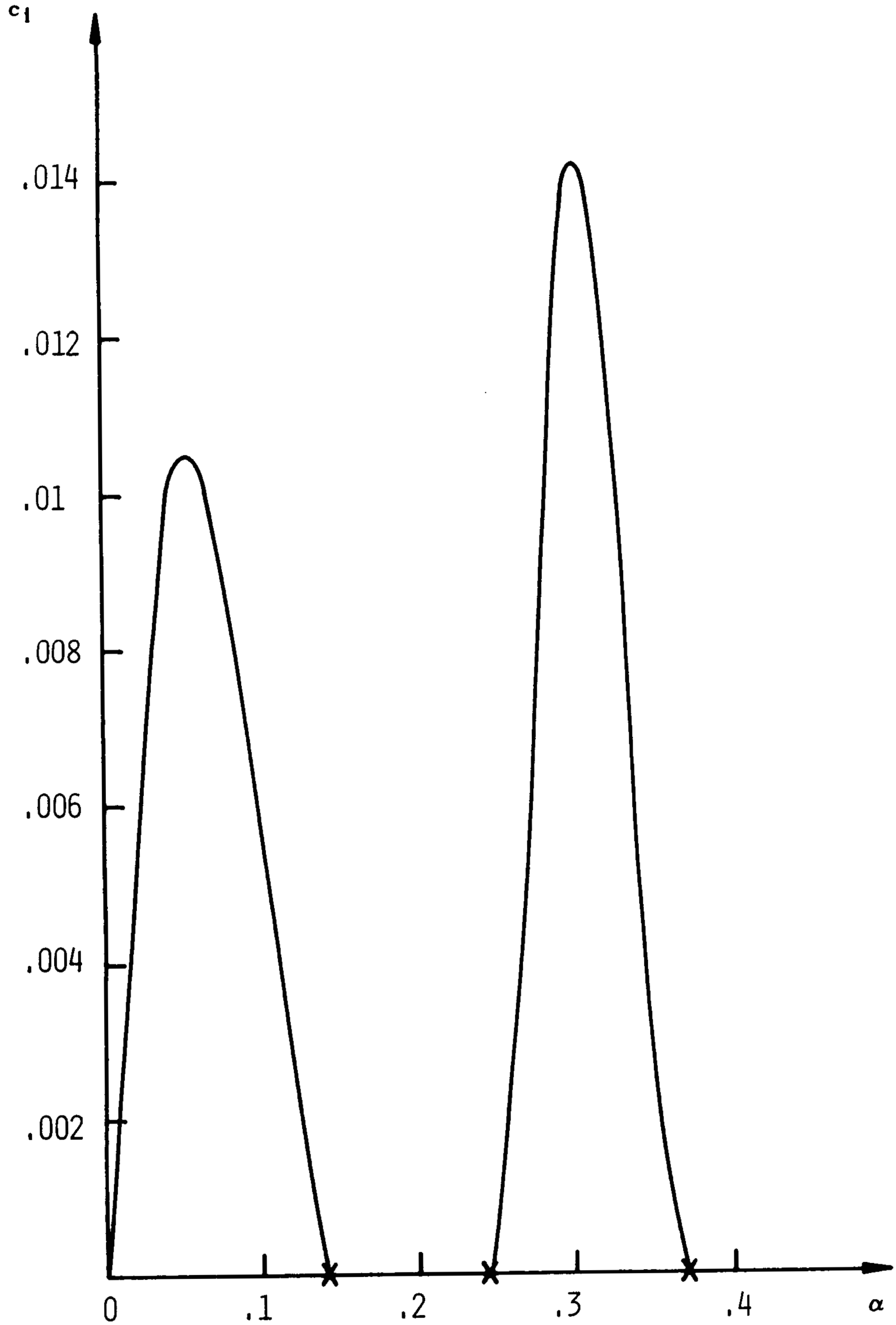

Fig 5a Variation of c_i with α, $M_\infty = 3.8$, $\zeta = 0$ (planar case)

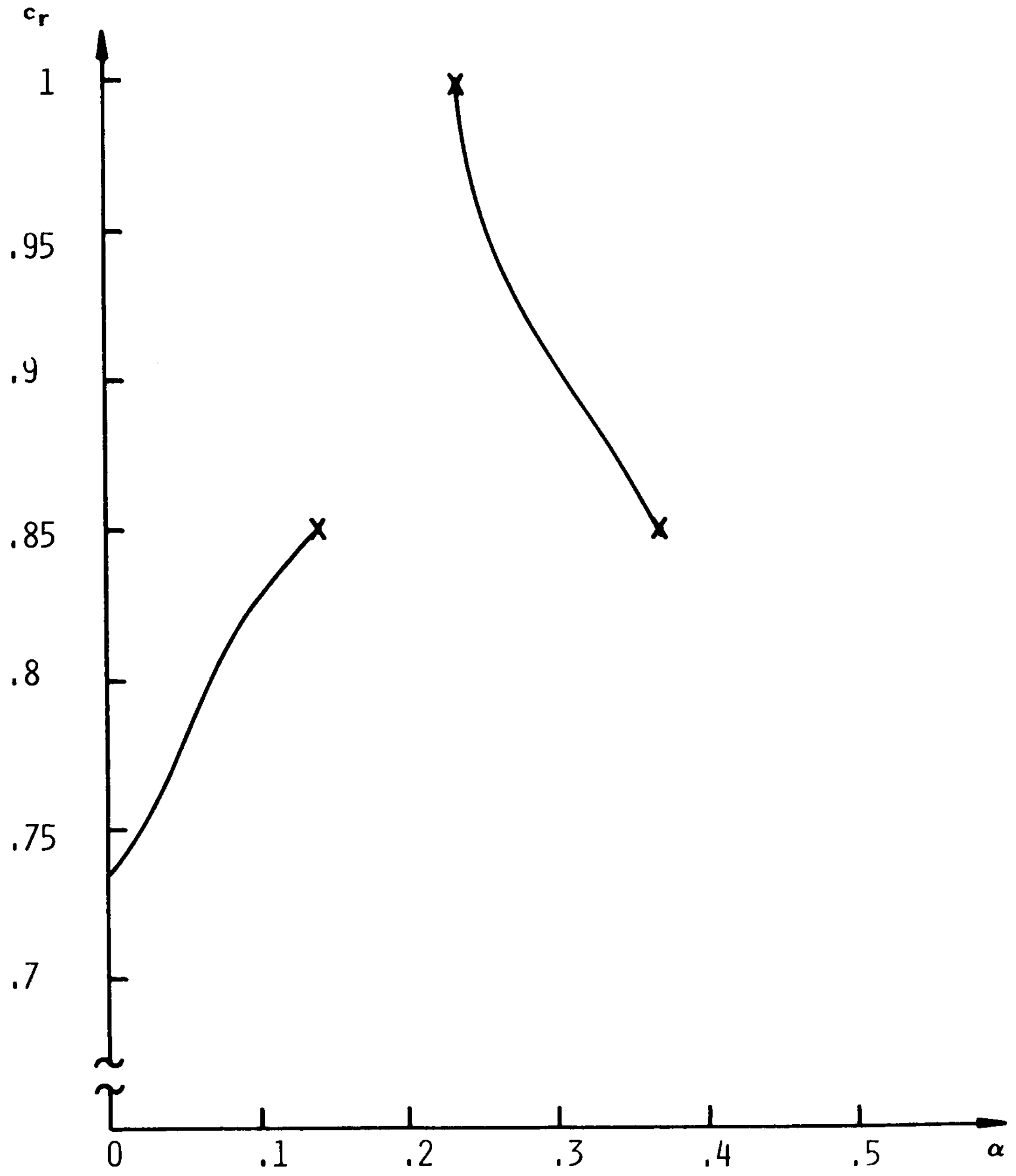

Fig 5b Variation of c_r with α, $M_\infty = 3.8$, $\zeta = 0$ (planar case)

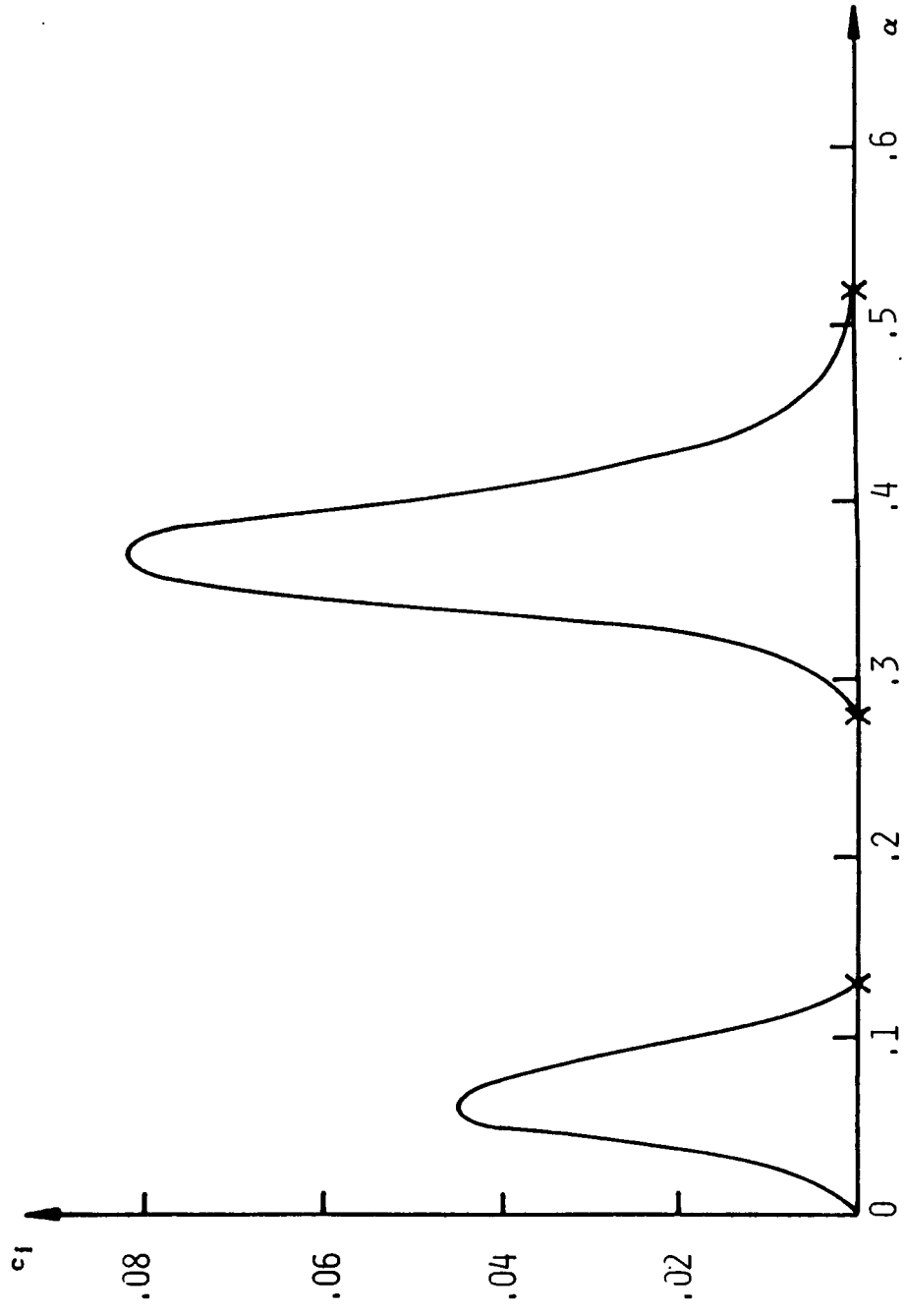

Fig 5c Variation of c_l with α, $M_\infty = 3.8$, $\zeta = 0.05$

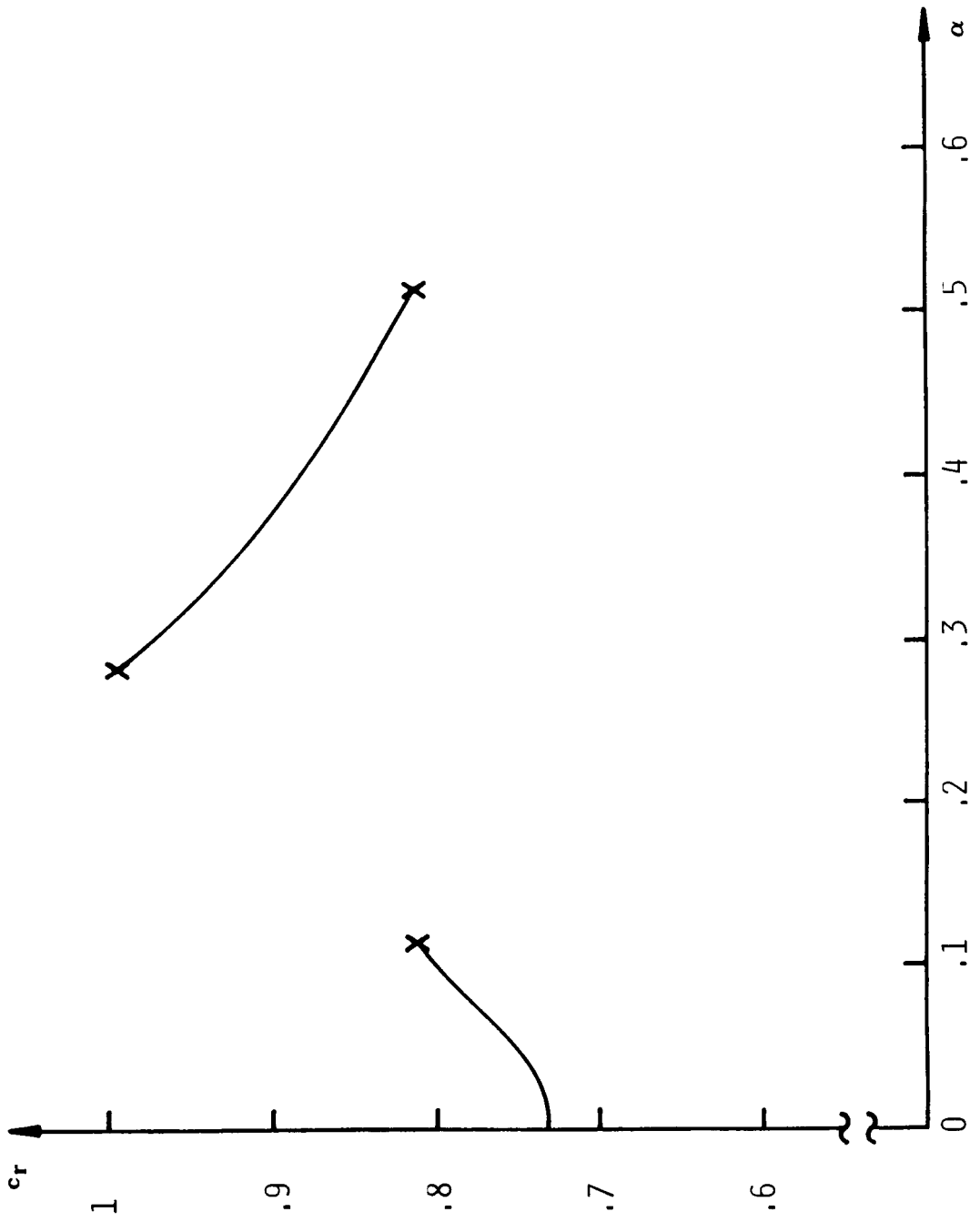

Fig 5d Variation of c_r with α, $M_\infty = 3.8$, $\zeta = 0.05$

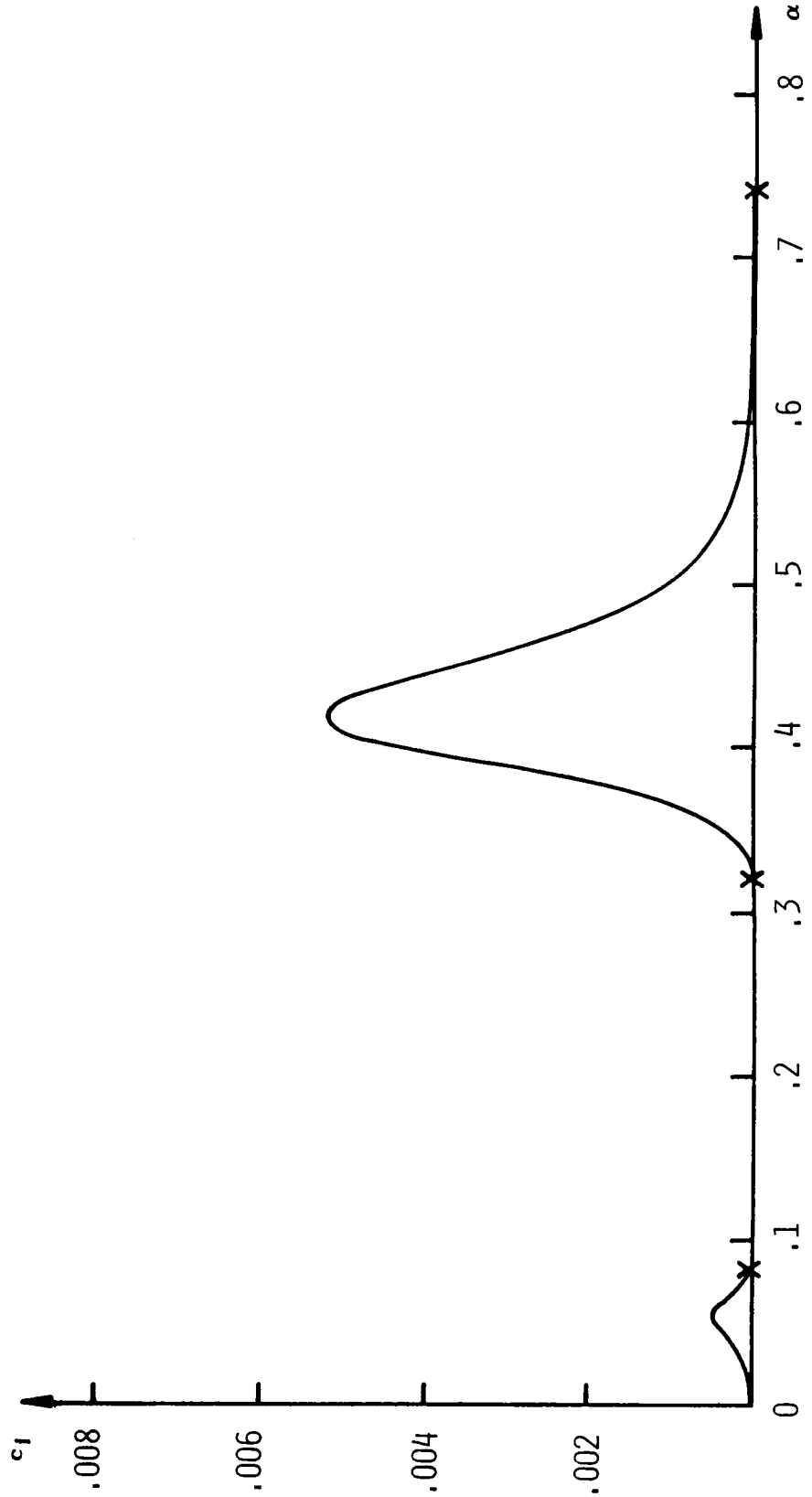

Fig 5e Variation of c_l with α, $M_\infty = 3.8$, $\varepsilon = 0.1$

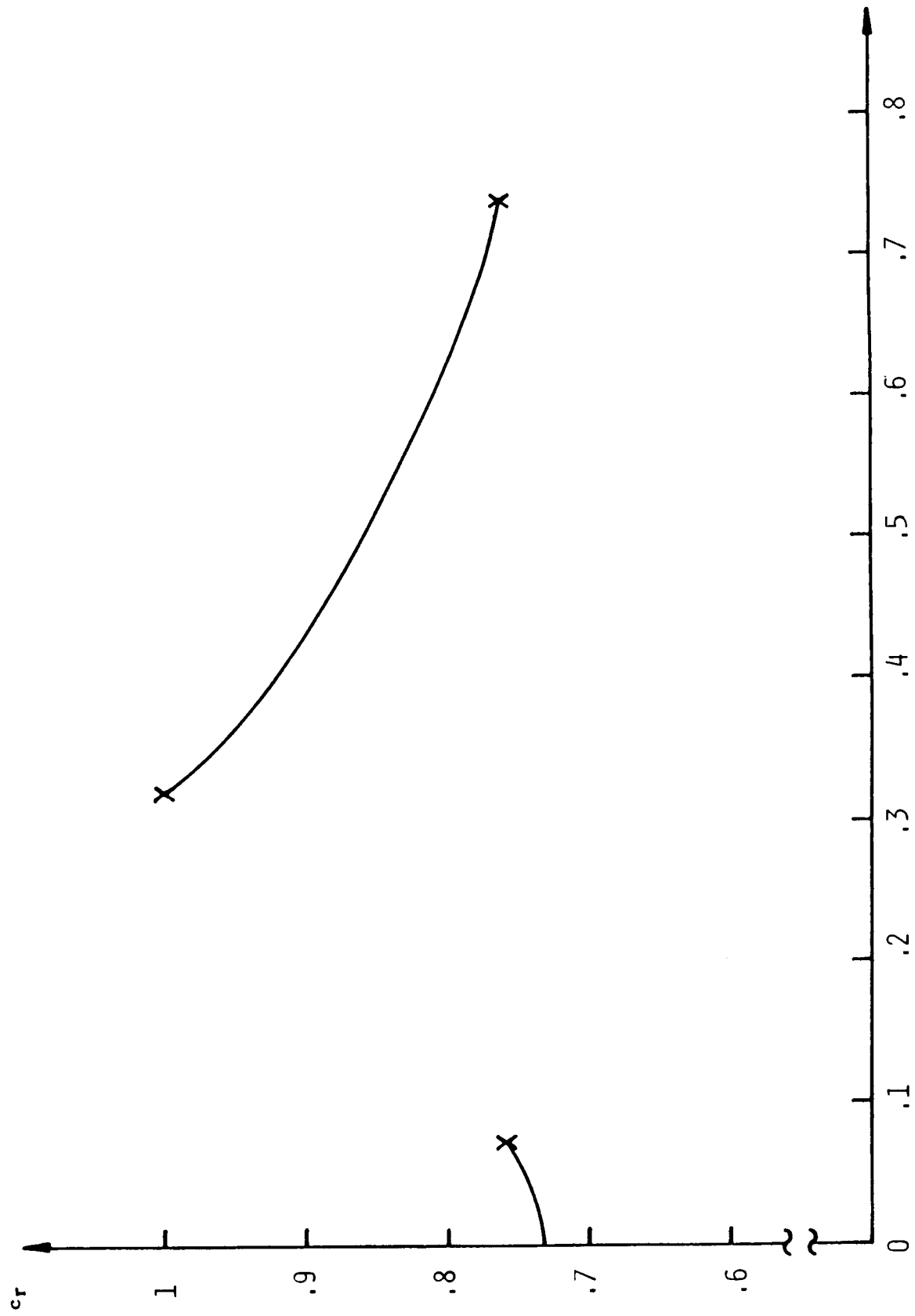

Fig 5f Variation of c_r with α, $M_\infty = 3.8$, $\tau = 0.1$

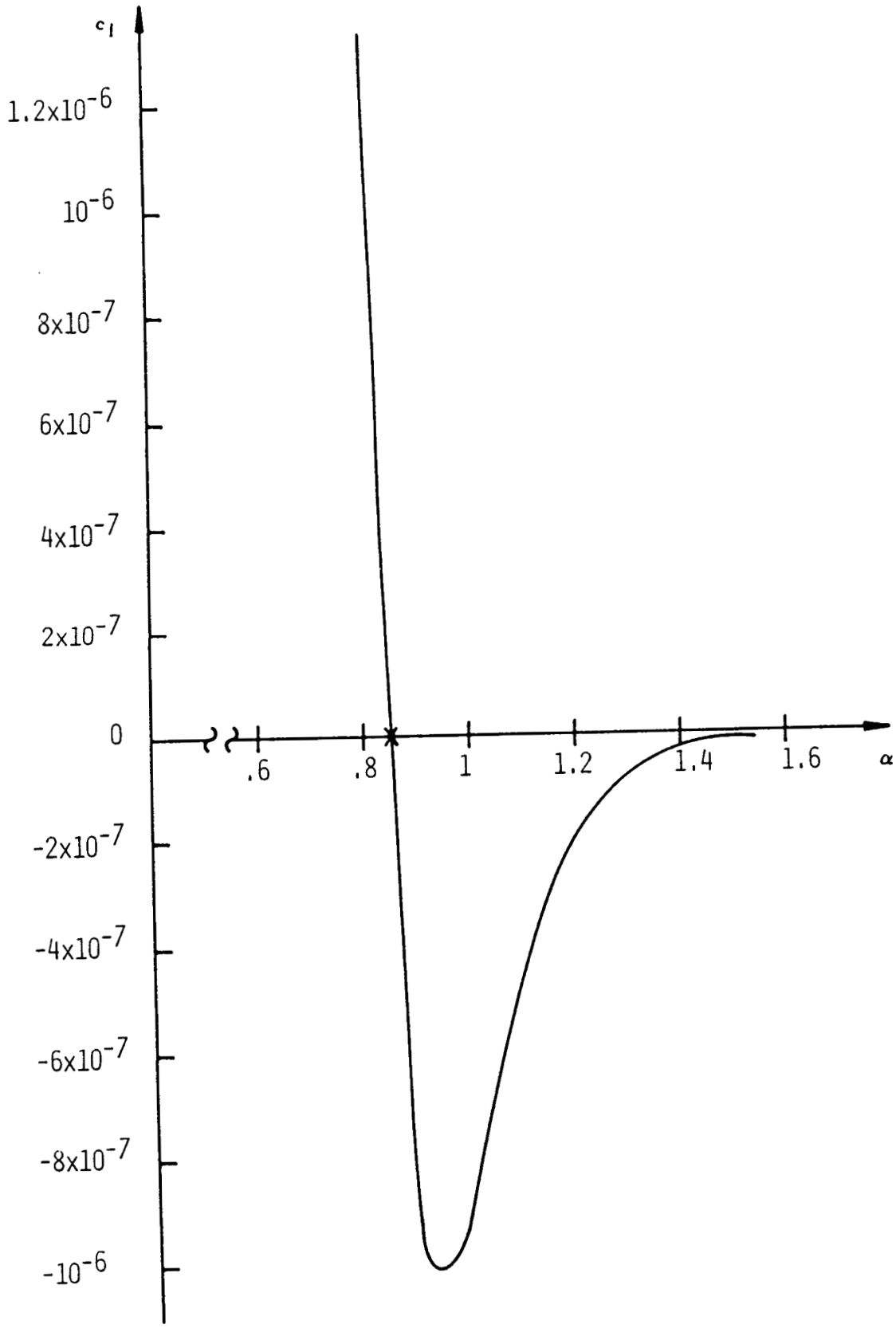

Fig 5g Variation of c_i with α, $M_\infty = 3.8$, $\gamma = 0.112$

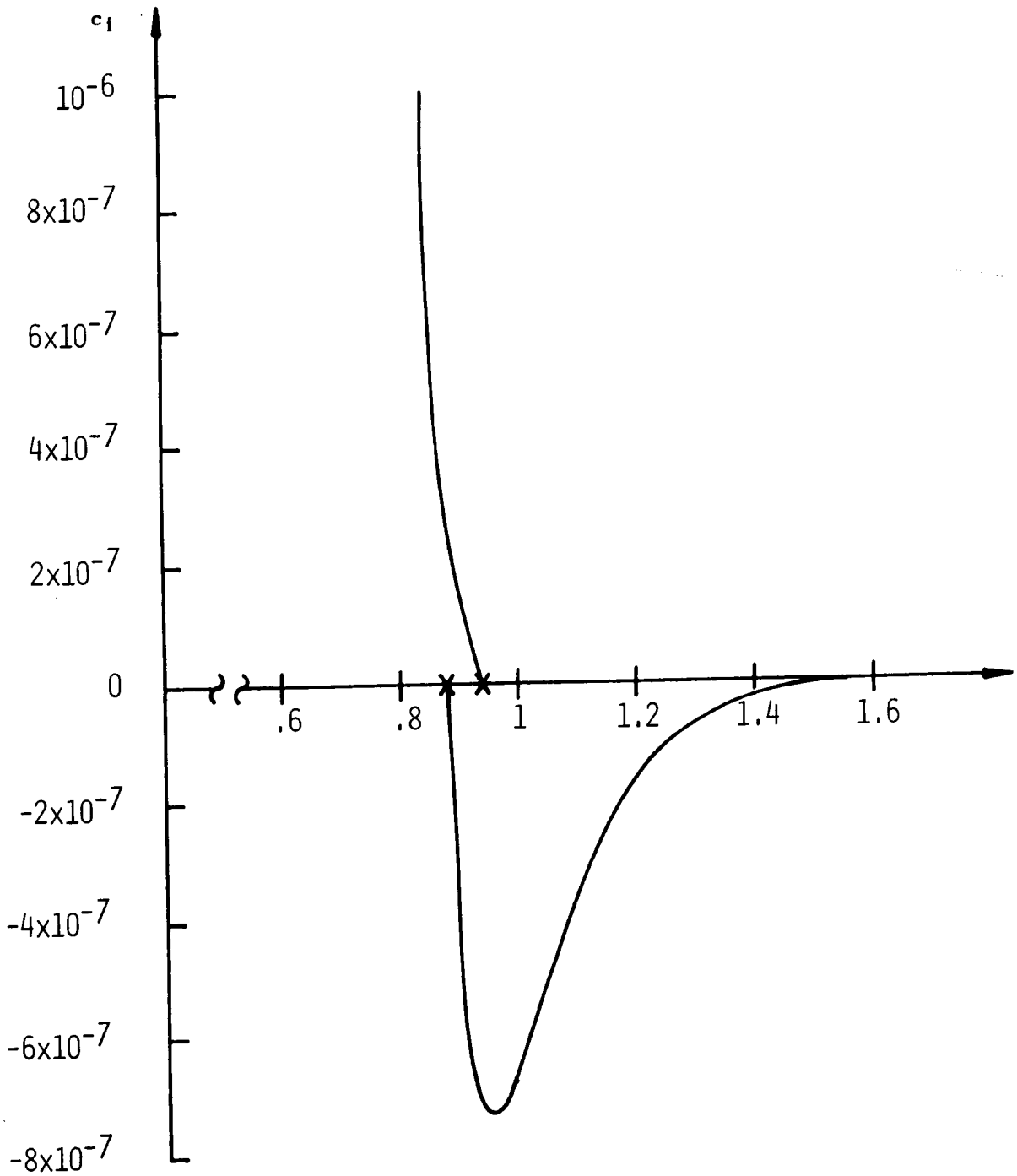

Fig 5h Variation of c_i with α, $M_\infty = 3.8$, $\zeta = 0.114$

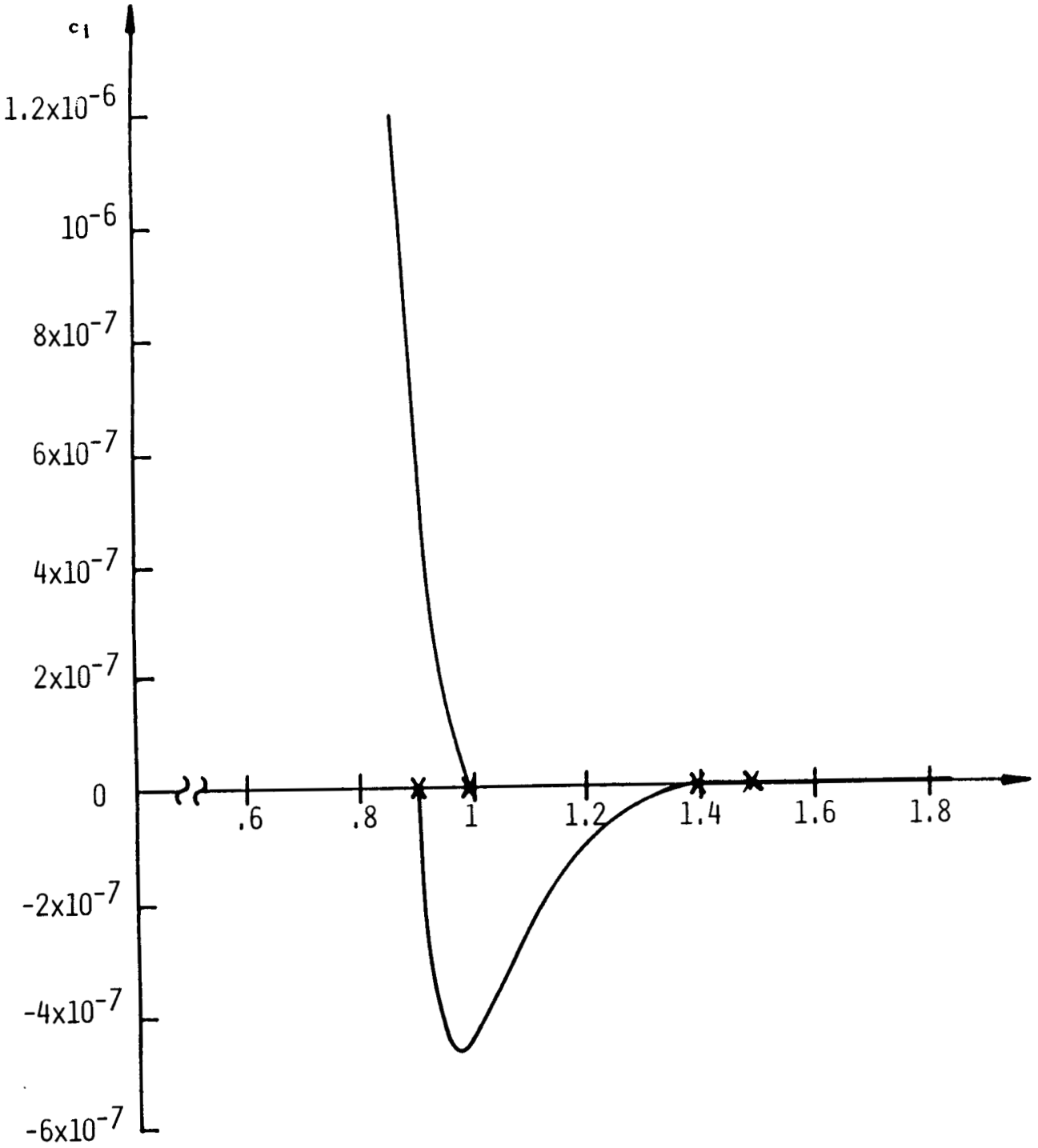

Fig 51 Variation of c_l with α, $M_\infty = 3.8$, $\tau = 0.116$

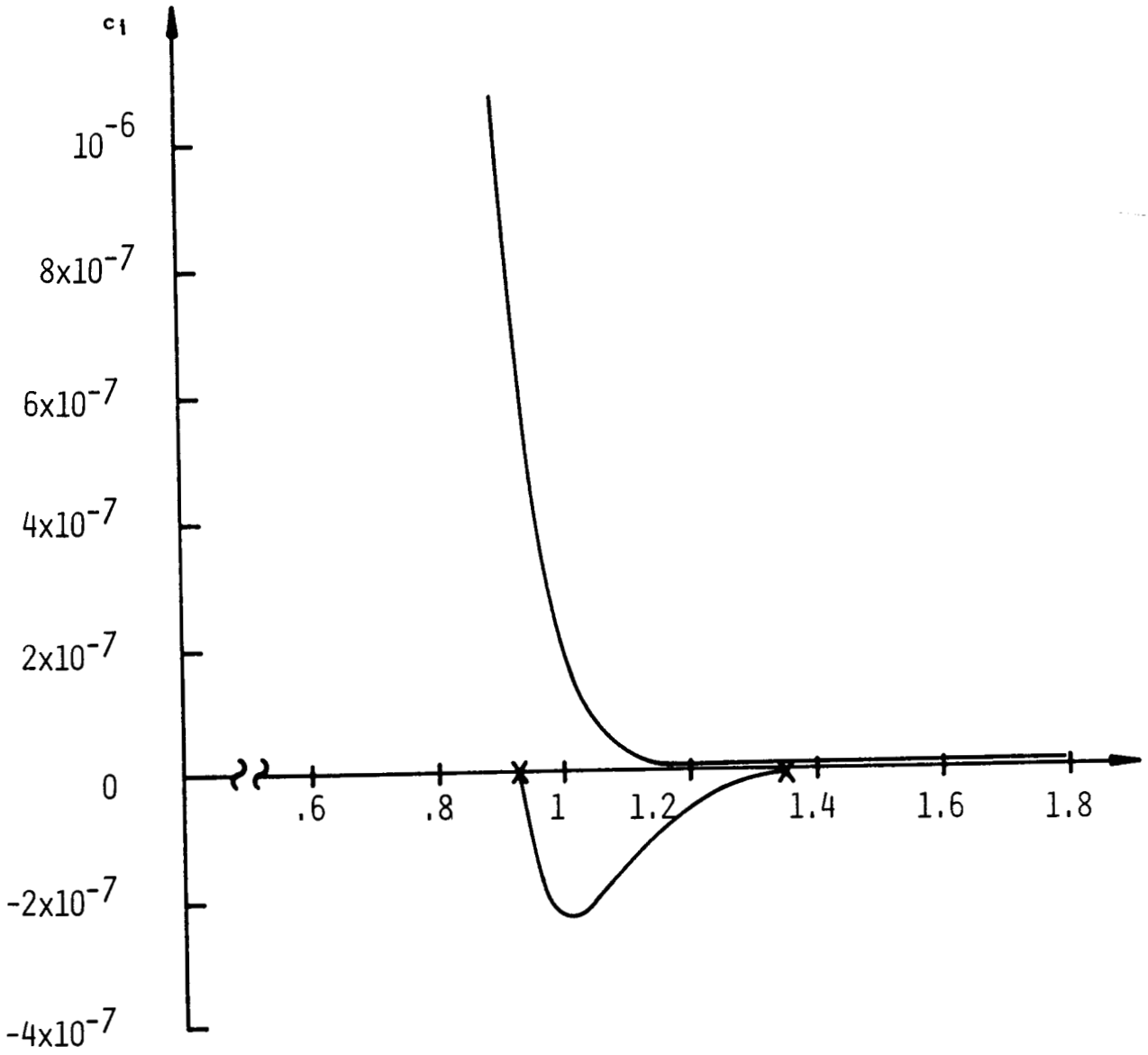

Fig 5j Variation of c_i with α, $M_\infty = 3.8$, $\delta = 0.118$

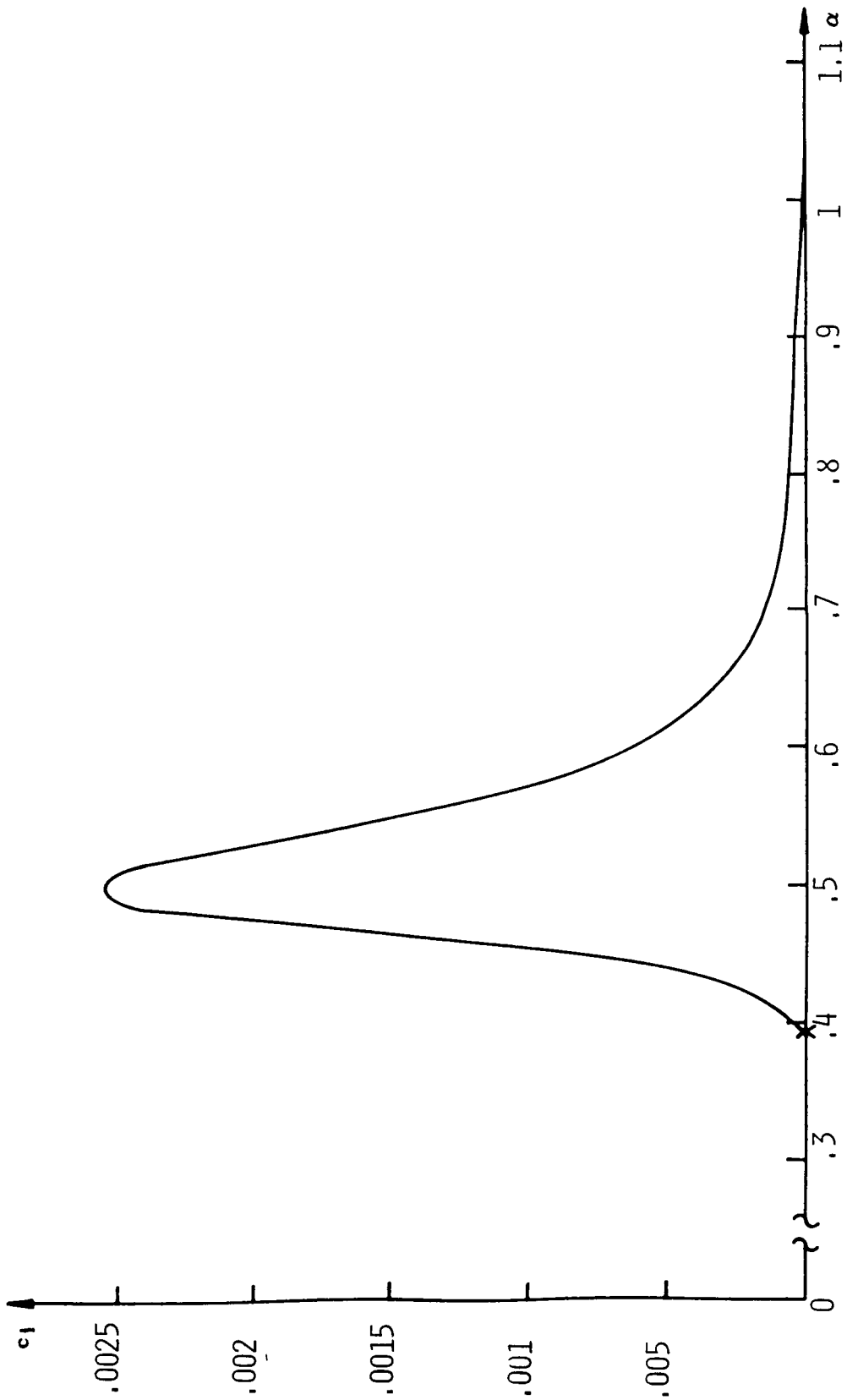

Fig 5k Variation of c_l with α, $M_\infty = 3.8$, $\bar{t} = 0.2$

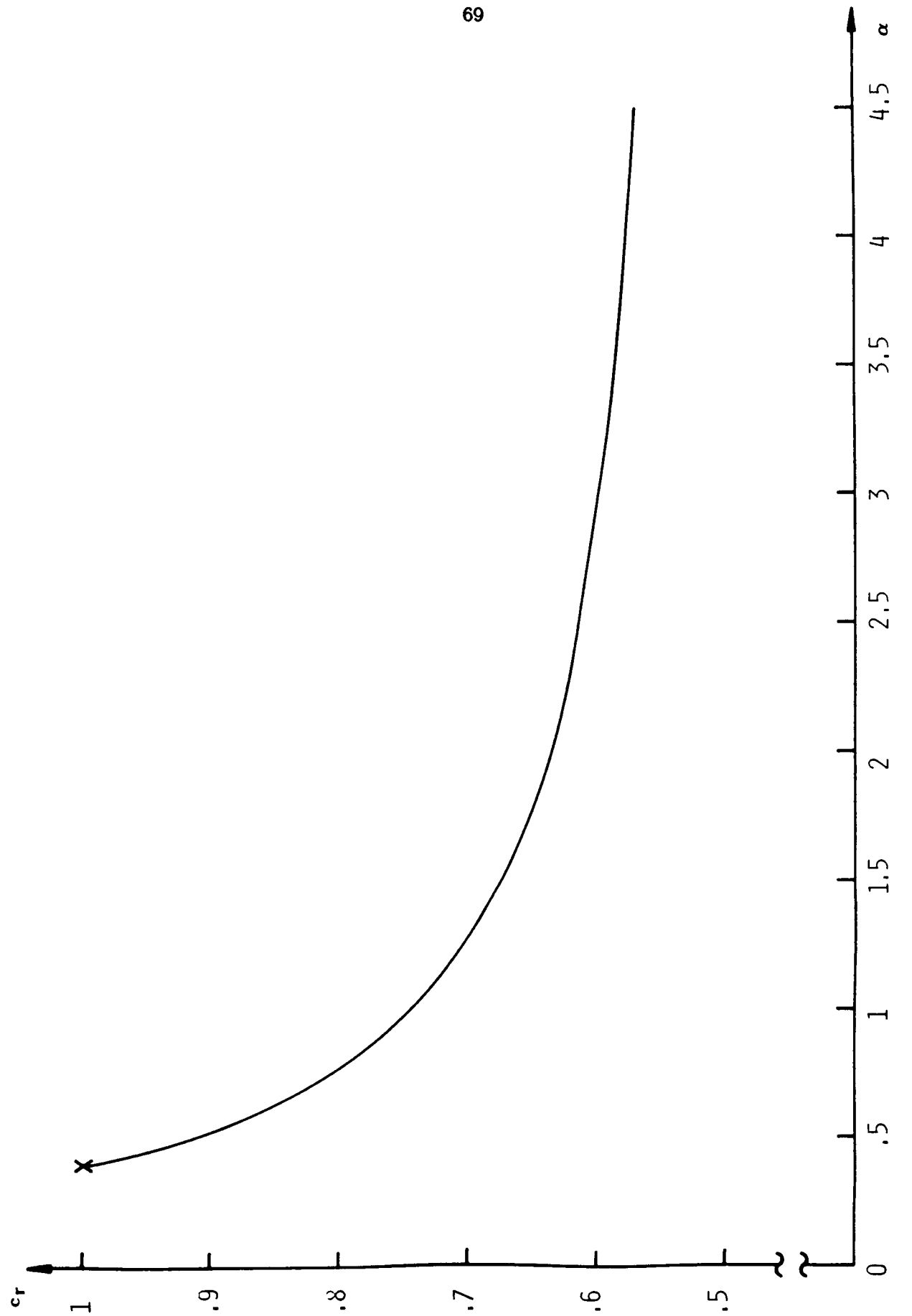

Fig 52 Variation of c_r with α, $M_\infty = 3.8$, $\tau = 0.2$

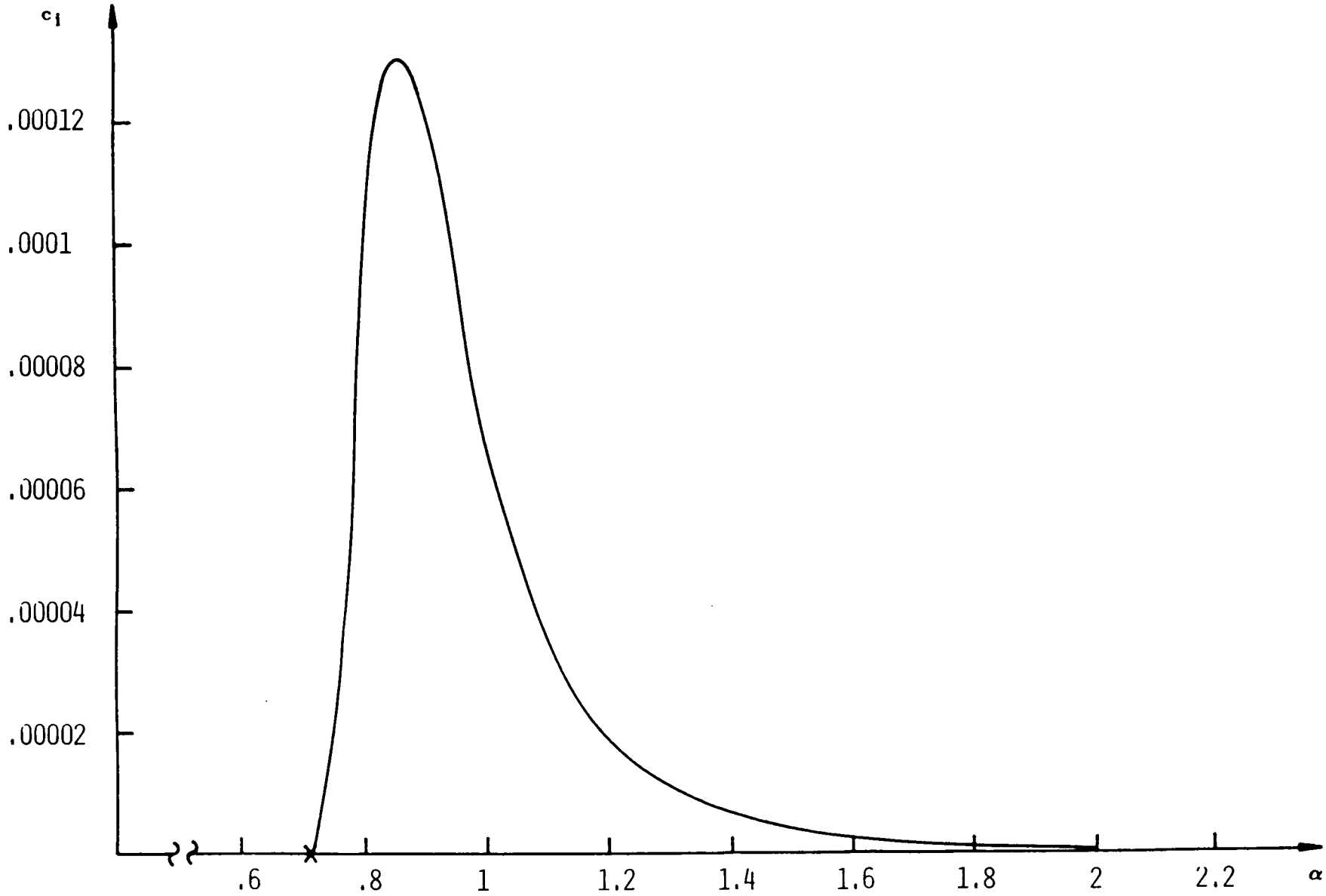

Fig 5m Variation of c_i with α, $M_\infty = 3.8$, $\zeta = 1.0$

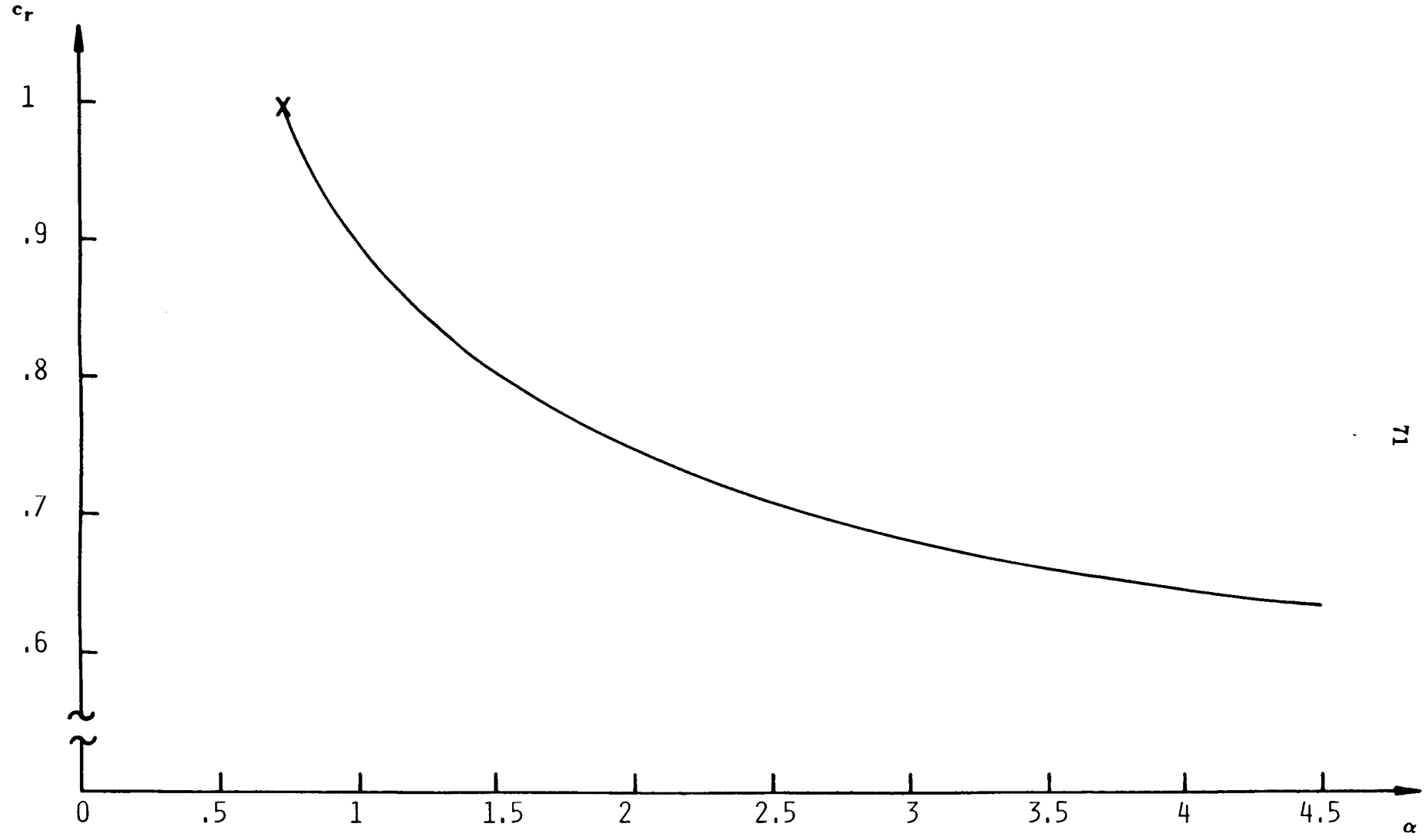

Fig 5n Variation of c_r with α, $M_\infty = 3.8$, $\gamma = 1.0$.

NASA
National Aeronautics and Space Administration

Report Documentation Page

1. Report No.	2. Government Accession No.	3. Recipient's Catalog No.
NASA CR-181816 ICASE Report No. 89-19		

4. Title and Subtitle	5. Report Date
THE INVISCID AXISYMETRIC STABILITY OF THE SUPERSONIC FLOW ALONG A CIRCULAR CYLINDER	February 1989
	6. Performing Organization Code

7. Author(s)	8. Performing Organization Report No.
Peter W. Duck	89-19
	10. Work Unit No. 505-90-21-01

9. Performing Organization Name and Address	11. Contract or Grant No.
Institute for Computer Applications in Science and Engineering Mail Stop 132C, NASA Langley Research Center Hampton, VA 23665-5225	NAS1-18605 NAS1-18107
	13. Type of Report and Period Covered Contractor Report
12. Sponsoring Agency Name and Address National Aeronautics and Space Administration Langley Research Center Hampton, VA 23665-5225	14. Sponsoring Agency Code

15. Supplementary Notes
Langley Technical Monitor: Richard W. Barnwell
Journal of Fluid Mechanics

Final Report

16. Abstract

The supersonic flow past a thin sraight circular cylinder is investigated. The associated boundary layer flow (i.e. the velocity and temperature field) is computed; the asymptotic, far downstream solution is obtained, and compared with the full numerical results.

The inviscid, linear, axisymmetric (temporal) stability of this boundary layer is also studied. A so called "doubly generalized" inflexion condition is derived, which is a condition for the existence of so called "subsonic" neutral modes. The eigenvalue problem (for the complex wavespeed) is computed for two freestream Mach numbers (2.8 and 3.8), and this reveals that curvature has a profound effect on the stability of the flow. The first unstable inviscid mode is seen to rapidly disappear as curvature is introduced, whilst the second (and generally the most important) mode suffers a substantially reduced amplification rate.

17. Key Words (Suggested by Author(s))	18. Distribution Statement
inviscid supersonic axisymmetric stability	02 - Aerodynamics Unclassified - Unlimited

19. Security Classif. (of this report)	20. Security Classif. (of this page)	21. No. of pages	22. Price
Unclassified	Unclassified	73	A04

NASA FORM 1626 OCT 86

NASA-Langley, 1989